Molecular Therapy
Methods & Clinical Development
Original Article

Role of Regulatory T Cell and Effector T Cell Exhaustion in Liver-Mediated Transgene Tolerance in Muscle

Jérôme Poupiot,[1] Helena Costa Verdera,[2] Romain Hardet,[2] Pasqualina Colella,[1] Fanny Collaud,[1] Laurent Bartolo,[3] Jean Davoust,[3] Peggy Sanatine,[4] Federico Mingozzi,[4,5] Isabelle Richard,[1,5] and Giuseppe Ronzitti[1,5]

[1]INTEGRARE, Genethon, INSERM, Univ Evry, Université Paris-Saclay, 91002 Evry, France; [2]UPMC, 75005 Paris, France; [3]UMR 1151, Necker-Institut Enfants Malades–Molecular Medicine Center, Paris, France; [4]Genethon, Evry, France

The pro-tolerogenic environment of the liver makes this tissue an ideal target for gene replacement strategies. In other peripheral tissues such as the skeletal muscle, anti-transgene immune response can result in partial or complete clearance of the transduced fibers. Here, we characterized liver-induced transgene tolerance after simultaneous transduction of liver and muscle. A clinically relevant transgene, α-sarcoglycan, mutated in limb-girdle muscular dystrophy type 2D, was fused with the SIINFEKL epitope (hSGCA-SIIN) and expressed with adeno-associated virus vectors (AAV-hSGCA-SIIN). Intramuscular delivery of AAV-hSGCA-SIIN resulted in a strong inflammatory response, which could be prevented and reversed by concomitant liver expression of the same antigen. Regulatory T cells and upregulation of checkpoint inhibitor receptors were required to establish and maintain liver-mediated peripheral tolerance. This study identifies the fundamental role of the synergy between Tregs and upregulation of checkpoint inhibitor receptors in the liver-mediated control of anti-transgene immunity triggered by muscle-directed gene transfer.

INTRODUCTION

The liver is one of the body's main biosynthetic organs, with key detoxifying functions enabled by efficient access to the systemic blood circulation and an intense metabolic activity. These characteristics make the liver an ideal target for gene replacement strategies. Results from clinical trials in hemophilia A and B support this point, establishing the safety and the efficacy of adeno-associated virus (AAV) vector-mediated gene transfer to human hepatocytes.[1,2] Another important feature of the hepatic environment is related to its pro-tolerogenic properties, initially described in the context of organ transplant.[3] This is consistent with the fact that liver, together with intestine, is the primary site of antigen presentation for food-derived proteins, and the presence of cells specialized in the control of immune responses results in what is known as an immune-privileged status. As a result, different hepatotropic viruses exploit the pro-tolerogenic milieu of the liver to persist and cause chronic diseases.[4]

Several mechanisms were reported to be responsible for the tolerogenic properties of the liver, e.g., the secretion of the pro-tolerogenic cytokines interleukin-10 (IL-10) and transforming growth factor β (TGF-β) by specialized antigen-presenting cells, the upregulation of inhibitory co-receptors, and the expansion of regulatory T cells (Tregs).[5] Tregs have a primary role in the control of humoral and cell-mediated immune responses against vector-encoded transgenes observed after liver gene transfer.[6,7] However, in the context of anti-transgene cytotoxic immune response, mechanisms other than Tregs induction are likely to be involved in the control of the immune response.[8]

Inhibitory co-receptors are part of a large family of co-receptors with a negative function on the activation of immune responses. After activation, the levels of these molecules on the surface of the immune cells increase, reflecting their role in the fine-tuning of the immune reactions to antigens. The impact of the expression of these molecules in the control of immune responses is particularly evident in chronic liver infections[9] and in tumors,[5] in which the expression of inhibitory co-receptor ligands mediates immune escape. A possible role for inhibitory co-receptors in the modulation of anti-transgene cytotoxic immune response via liver gene transfer has been hypothesized, although a direct characterization of the phenomenon is still missing.[10,11]

Differently from what was observed in the liver,[6,12,13] AAV-mediated gene transfer after intramuscular injection may result in the development of anti-transgene immune responses.[14] Expansion of antigen-specific *CD8*$^+$ T cells has been associated with the clearance of transduced fibers both in preclinical and clinical studies.[15–17] Like in the case of muscular dystrophies, in which Tregs have been documented to home to the inflamed muscle,[18,19] AAV-triggered cytotoxic immune responses are balanced by Tregs able to partially control anti-transgene immune responses.[20] Early findings demonstrated that

Received 23 August 2019; accepted 26 August 2019;
https://doi.org/10.1016/j.omtm.2019.08.012.

[5]These authors contributed equally to this work.

Correspondence: Giuseppe Ronzitti, Genethon, 1 bis rue de l'internationale, 91000 Evry, France.
E-mail: gronzitti@genethon.fr

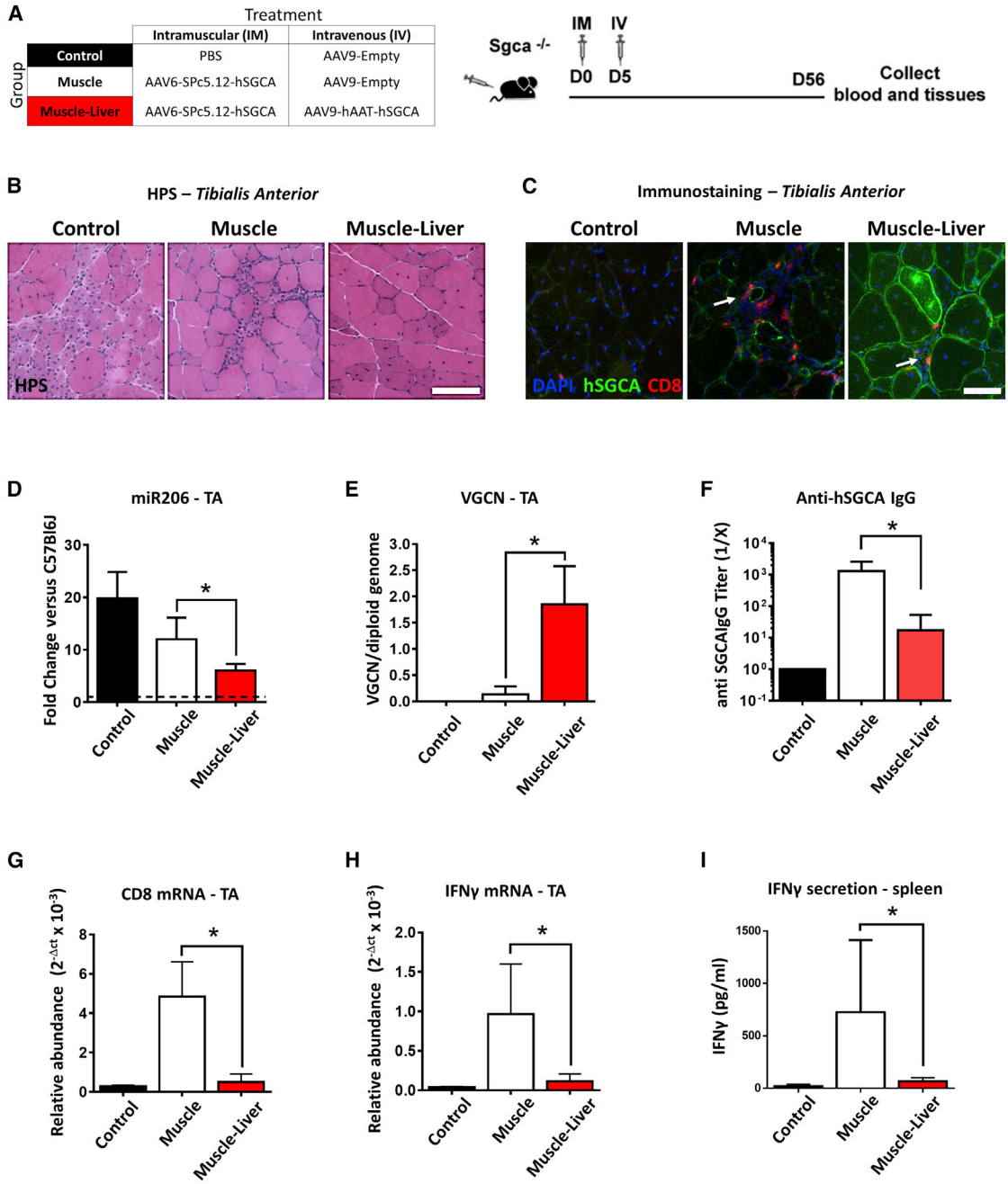

Figure 1. Simultaneous Liver and Muscle Targeting Improves Transgene Expression in Dystrophic Muscle

(A) Five-week-old *Sgca*$^{-/-}$ mice were intramuscularly (i.m.) injected (tibialis anterior [TA]) at day (D) 0 with 5×10^9 vg/mouse of AAV6-SPc5.12-hSGCA vector. Five days after intramuscular injection, mice received an intravenous injection (IV) with either 5×10^{11} vg/mouse of AAV9-hAAT-hSGCA (Muscle-Liver group) or an empty AAV9 vector (Muscle group). In parallel, a group of mice injected intramuscularly with PBS and intravenously with the empty AAV9 vector was used as control (Control group). Two months after treatment, mice were sacrificed, and tissues were collected. (B) Hematoxylin phloxine saffron staining (HPS; upper panel; scale bar: 100 μm) performed in TA. (C) Immunostaining with anti-hSGCA (green), CD8 (red), and DAPI (blue) performed in TA. White arrows indicate CD8 cells. Scale bar: 50 μm. (D) miR-206 levels measured in TA and represented as fold-change versus wild-type C57BL/6J mice (dotted line in the graph). (E) Vector genome copy number (VGCN) per diploid genome measured in TA. (F) Anti-hSGCA IgG titers measured by ELISA using recombinant hSGCA protein. (G and H) CD8 (G) and IFN-γ (H) mRNA measured in TA. (I) IFN-γ secretion from recombinant hSGCA-stimulated splenocytes measured by ELISA. Data were expressed as mean ± SD. Statistical analyses were performed by Student's t test in (D), (E), and (G)–(I); a non-parametric Mann-Whitney test was used for (F) (*$p < 0.05$, †$p < 0.05$ as indicated, n = 2 for Control group, n = 4 for Muscle group, and n = 6 for Muscle-Liver group).

the simultaneous liver and muscle targeting is able to control the humoral and cell-mediated anti-transgene immune responses.[21,22]

Here, we characterized the liver-mediated control of anti-transgene immune response resulting from the intramuscular injection of an AAV vector expressing human α-sarcoglycan (hSGCA). This protein, mutated in limb-girdle muscular dystrophy type 2D, when expressed in *Sgca*$^{-/-}$ muscle, induces a strong anti-transgene immune response resulting in fiber loss and transgene clearance.[23]

We found that concomitant liver and muscle expression of hSGCA was able to control the anti-transgene immune response even when this immune response was established ahead of liver gene transfer. Then, using a model antigen derived from hSGCA, we characterized in detail the cytotoxic anti-transgene immune response. Importantly, by taking advantage of antibodies specifically depleting Tregs or inhibiting the interactions between inhibitory co-receptors and their ligands, we dissected the synergistic role of these mechanisms in the control of the immune response in the setting of concomitant AAV-mediated liver and muscle gene transfer.

RESULTS

Liver Gene Transfer Controls Cytotoxic Transgene-Specific Immune Responses Resulting from Intramuscular Injection in Dystrophic Mice

AAV-mediated liver gene transfer induces a strong peripheral tolerance likely to control the anti-transgene immune responses at a systemic level.[12,24] Here, we challenged the robustness of this mechanism in a dystrophic mouse model characterized by muscle inflammation and known to mount significant immune responses against the human SGCA protein.[25] Tibialis anterior (TA) muscle of *Sgca*$^{-/-}$ mice was injected intramuscularly (i.m.) with vehicle (PBS, Control group) or with an AAV6 vector expressing hSGCA under the control of the muscle promoter SPc5.12. Five days later, mice received by a systemic route either empty AAV9 capsids (Muscle group) or an AAV9 vector expressing the hSGCA transgene under the control of human alpha-1-anti-trypsin (hAAT) liver-specific promoter (Muscle-Liver group; Figure 1A). Two months after vector injection, the expression of hSGCA transgene in the liver of Muscle-Liver-injected animals was confirmed by qRT-PCR and immunostaining (Figures S1A and S1B). A significant enhancement in muscle transduction and consequent muscle structure normalization were observed in the Muscle-Liver group compared with the Muscle group as shown by immunohistochemistry (Figure 1B), anti-hSGCA immunostaining (Figure 1C), and miR-206 expression (Figure 1D), a marker of regeneration in muscle.[26] The quantification of the vector genome copy number (VGCN) per diploid genome confirmed the improved transduction in muscle of animals of the Muscle-Liver group ($p < 0.01$ versus the Muscle group; Figure 1E). Animals receiving the vector intramuscularly (Muscle group) also developed a robust anti-hSGCA humoral immune response, which was significantly reduced in the Muscle-Liver-treated group ($p < 0.05$; Figure 1F). The inhibition of the anti-hSGCA humoral response was associated with a reduction of activated *CD8*$^{+}$ cells infiltrating the injected muscle of Muscle-Liver-treated animals, as confirmed by immunohistochemistry (Figure 1C) and mRNA expression of inflammatory markers CD8 and interferon gamma (IFN-γ) in the same group ($p < 0.001$ and $p < 0.05$ versus Muscle, respectively; Figures 1G and 1H). Increased secretion of IFN-γ from hSGCA protein-stimulated splenocytes extracted from mice of the Muscle group compared with the Muscle-Liver group ($p < 0.05$; Figure 1I) was also observed.

These results demonstrate that liver gene transfer induces a dominant peripheral tolerance to a human transgene expressed in a dystrophic muscle. This represents a particularly stringent setting because the fragility of the muscle fibers, consequent to the lack of SGCA protein in the dystrophin complex, induces a persistent inflamed state in the muscle that enhances anti-transgene immune responses.[17,27]

Liver Expression of hSGCA Prevents and Reverses the Loss of Transduced Fibers in Muscle of Wild-Type Mice

To evaluate whether wild-type mice had an anti-hSGCA immune response similar to that observed in KO animals, we injected 8-week-old C56BL6 mice intramuscularly with a vector expressing hSGCA under the control of the SPc5.12 promoter (Figure S2A). Mice were sacrificed 5, 15, and 30 days after vector injection. Histological analysis indicated the presence of *CD8*$^{+}$ T cell infiltrates in the muscle, consistent with an ongoing immune response (Figure S2B). CD8 mRNA levels in muscle extracts were increased compared with PBS-injected mice at days 15 and 30 ($p < 0.001$ versus Control [CTRL]), whereas IFN-γ mRNA levels were increased 15 days after vector injection ($p < 0.0001$ versus Control; Figures S2C and S2D). Decreased VGCNs were observed 15 and 30 days after vector injection ($p < 0.0001$ versus day [D] 5), suggesting that the ongoing transgene immune response resulted in clearance of the vector from transduced muscle fibers (Figure S2E). Of note, a separate control cohort of mice injected with an AAV6 vector expressing murine-secreted alkaline phosphatase at the same dose did not show any sign of inflammation (data not shown). These results suggest that AAV-mediated expression of hSGCA is immunogenic in wild-type mice regardless of the endogenous expression of murine SGCA.

The presence of an immune response in wild-type mice offered the possibility to investigate the liver-mediated control of the anti-hSGCA immune response without the confounding effect of immune signals because of the dystrophic process ongoing in *Sgca*$^{-/-}$ mice. C57BL/6J mice were injected intramuscularly with an AAV6-SPc5.12-hSGCA vector and then received a systemic injection of an AAV9 vector expressing the same transgene under the transcriptional control of the liver-specific promoter hAAT. This second vector administration was performed either on the same day (Muscle-Liver day 0) or 15 days after (Muscle-Liver day 15) intramuscular injection (Figure 2A) at the peak of muscle inflammation as observed in Figure S2. One month after vector injection, hSGCA was expressed in the liver of mice of the Muscle-Liver day 0 and day 15 groups at similar levels (Figure S2F). As expected, animals injected intramuscularly with the AAV6-SPc5.12-hSGCA vector alone showed increased levels of *CD8*$^{+}$ infiltrates, whereas the concomitant systemic injection

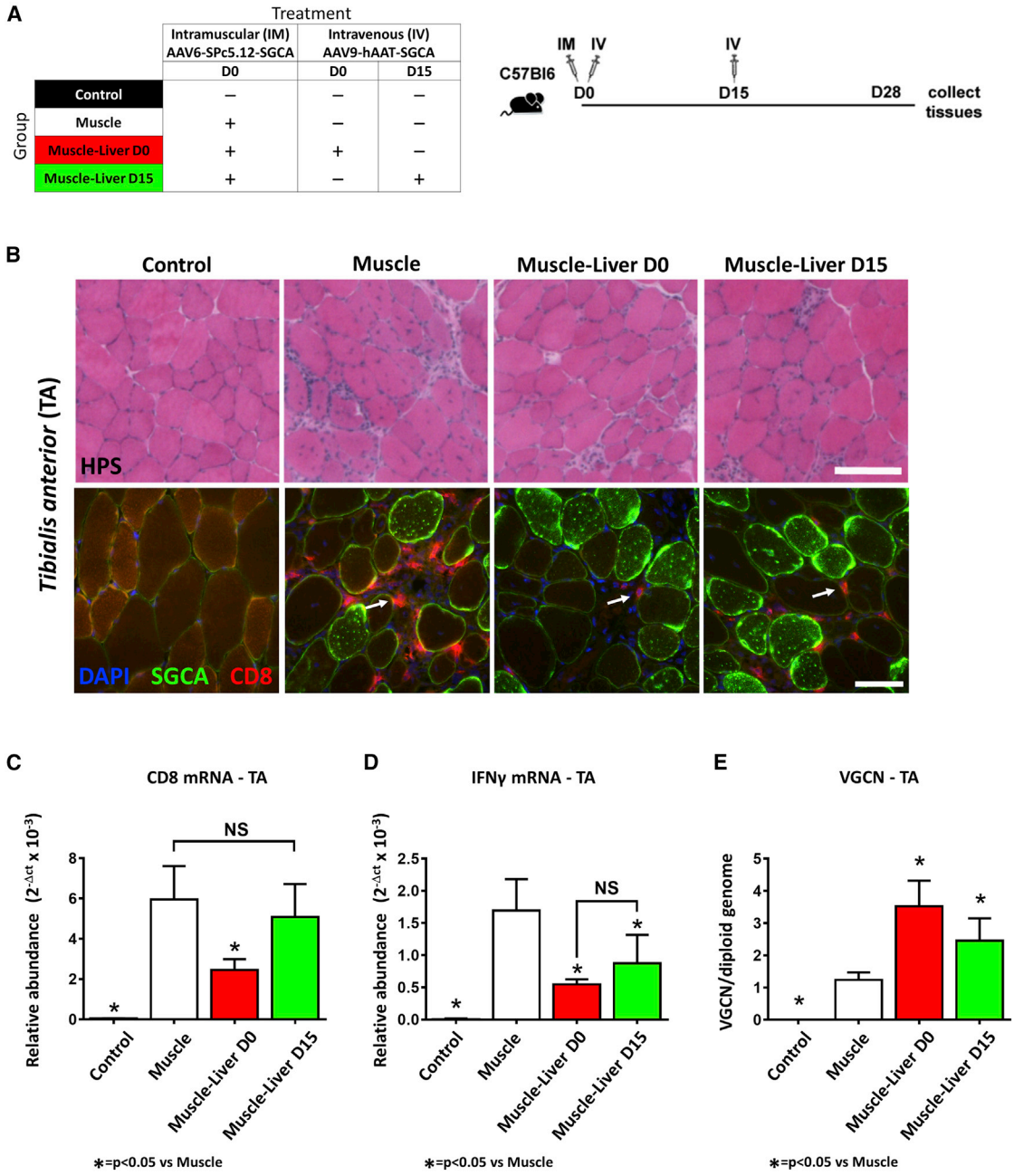

Figure 2. Liver Transduction Controls Preexisting Anti-hSGCA Immune Response in C57BL/6J Mice

(A) Eight-week-old C57BL/6J mice received at day 0 an intramuscular injection (TA) of 2.5 × 10^9 vg/mouse of AAV6-SPc5.12-hSGCA vector and at day 0 or day 15 an intravenous injection (IV) of 1 × 10^{11} vg/mouse of AAV9-hAAT-SGCA (Muscle-Liver day 0 and Muscle-Liver day 15, respectively). In parallel, two groups of mice injected intramuscularly at day 0 with PBS or 2.5 × 10^9 vg/mouse of AAV6-SPc5.12-hSGCA vector were used as controls (Control and Muscle groups, respectively). One month after treatment, mice were sacrificed and tissues collected. (B) HPS (upper panel, scale bar: 100 μm) and anti-hSGCA (green), CD8 (red), and DAPI (blue) immunostaining (lower panel, scale bar: 50 μm) performed on TA muscle. White arrows indicate CD8 cells. (C and D) CD8 (C) and IFN-γ (D) mRNA measured in TA. (E) Vector genome copy number (VGCN) per diploid genome measured in TA. Data were expressed as mean ± SD. Statistical analyses were performed by ANOVA (*p < 0.05; n = 4 per group).

of the liver-expressing vector reduced the level of infiltrates, in particular when the two vectors were administered at the same time point (Figure 2B). Analysis of the levels of expression of CD8 mRNA in the muscle confirmed the reduction of CD8-expressing cells in mice co-injected in muscle and liver at day 0 ($p < 0.01$ versus the Muscle group), but not at day 15 (Figure 2C). Interestingly, the levels of

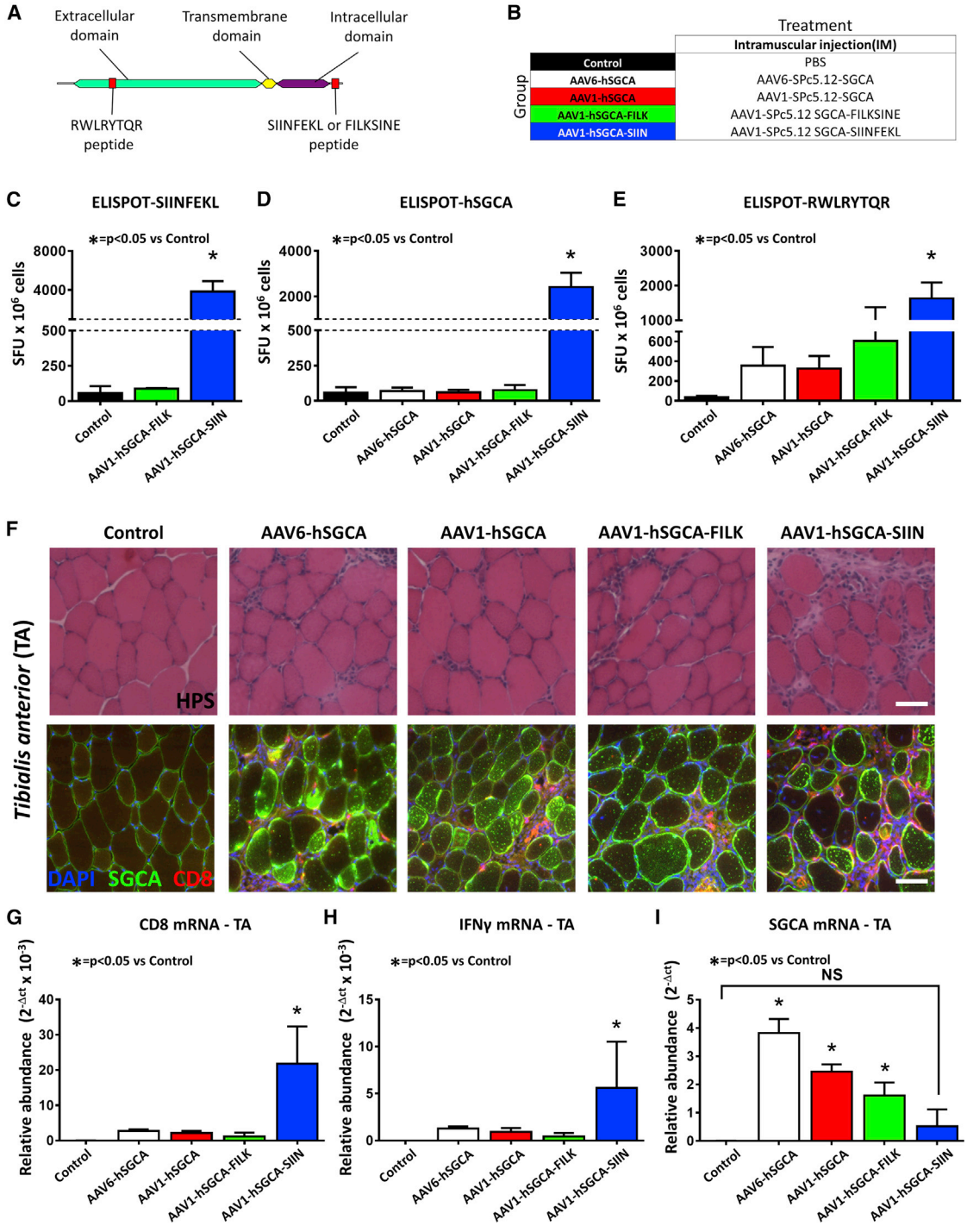

Figure 3. hSGCA-SIIN Fusion Transgene as a Model Antigen to Evaluate Cytotoxic Response in C57BL/6J Mice

(A) Schematic representation of the fusion between hSGCA and SIINFEKL epitope. The SIINFEKL peptide and its scrambled version FILKSINE were fused to the C-terminal domain of hSGCA (hSGCA-SIIN and hSGCA-FILK, respectively). RWLRYTQR peptide located in the extracellular domain was top-score predicted for binding on murine H-2Kb MHC class I. (B) Five-week-old C57BL/6J mice were intramuscularly injected (TA) with 1×10^{10} vg/mouse of AAV1- or AAV6-expressing hSGCA under the SPc5.12-promoter (AAV1-hSGCA, AAV6-hSGCA) or with the same dose of an AAV1 vector expressing either the hSGCA-SIIN fusion protein (AAV1-hSGCA-SIIN) or the hSGCA-FILK fusion protein (AAV1-hSGCA-FILK) under the control of the same promoter. In parallel, one group of mice was injected intramuscularly with PBS as control (Control group).

(legend continued on next page)

IFN-γ mRNA were similar between Muscle-Liver day 0 and day 15 groups and significantly reduced compared with the Muscle group ($p < 0.05$; Figure 2D). The decreased immune reaction was associated with an improved transduction of muscle fibers of mice of the Muscle-Liver day 0 and day 15 groups as measured by VGCN analysis ($p < 0.001$ and $p < 0.05$ versus Muscle only, respectively; Figure 2E).

We then measured the levels of expression of a panel of mRNAs of immune-related genes in the liver of treated mice (Table S1). Consistent with previous reports of antigen-independent homing of activated T cells in the liver,[28] CD4 mRNA levels were significantly increased in the liver of mice intramuscularly treated with the AAV6- SPc5.12-hSGCA vector, which experienced the highest inflammation levels. Conversely, in mice treated with both muscle and liver vectors simultaneously or 15 days apart, the upregulation of genes associated with tolerance and T cell exhaustion such as FoxP3 and programmed cell death ligand 1 (PD-L1) was noted, as well as the increase of CD8 expression, suggesting homing of CD8 T cells in the liver (Table S1).

These data confirm that liver-targeted expression of hSGCA is able to control the induction of anti-hSGCA immune response following intramuscular administration. Importantly, the results for the day 15 group indicate that liver transduction is able to control, at least partially, an already established immune response. Liver T cell homing and upregulation of immunomodulatory genes appear to be signatures of the phenomenon.

Muscle Expression of the SIINFEKL-hSGCA Fusion Protein Is Highly Immunogenic and Allows Tracking of Transgene-Specific T Cell Responses

Based on the results in *Sgca*$^{-/-}$ and wild-type mice, we then better characterized the cytotoxic response to the hSGCA transgene. To evaluate the activation of antigen-specific T cells, we fused the C terminus of the protein with a portion of the ovalbumin protein containing the major histocompatibility complex (MHC) class I-specific[29] epitope SIINFEKL (hSGCA-SIIN; Figure 3A). As a control of the specificity of the immune response, hSGCA was fused with a scrambled version of the SIINFEKL peptide, FILKSINE (hSGCA-FILK). C57BL/6J mice were injected intramuscularly with AAV1 or AAV6 vectors expressing hSGCA or with AAV1 vectors expressing hSGCA-SIIN or hSGCA-FILK under the control of the SPc5.12 promoter (Figure 3B). Fifteen days after the injection, mice were sacrificed, and the activation of T cells was tested by IFN-γ enzyme-linked immunospot (ELISPOT). As expected, the stimulation of splenocytes with the SIINFEKL peptide led to a robust activation in mice injected with AAV1 vectors expressing hSGCA-SIIN, but not with hSGCA-FILK ($p < 0.05$ versus Control; Figure 3C). When the stimulation was performed with the hSGCA recombinant protein (Figure 3D), we observed a robust T cell activation only in the group injected with the SGCA-SIIN antigen ($p < 0.05$ versus Control, respectively). Interestingly, the stimulation with a peptide epitope derived from hSGCA and predicted to bind to MHC class I (Figure 3E; Figure S3) induced a general increase in the IFN-γ ELISPOT spot counts in all of the groups injected with vectors expressing hSGCA. However, statistical significance was reached only in the group injected with the hSGCA-SIIN fusion protein ($p < 0.01$ versus Control, respectively). No differences were observed between AAV1 and AAV6 serotypes. The injection of the hSGCA-SIIN-expressing vector also resulted in increased muscle *CD8*$^{+}$ T cell infiltrates as visualized by hematoxylin phloxine saffron (HPS) staining and immunofluorescence (Figure 3F). These results were also confirmed by the increased levels of CD8 and IFN-γ mRNA in the hSGCA-SIIN-injected muscle ($p < 0.0001$ and $p < 0.05$ versus Control, respectively; Figures 3G and 3H). These results indicate that the hSGCA-SIIN fusion protein is highly immunogenic and allows tracking of transgene-specific immune responses both to SIINFEKL and hSGCA. Fifteen days after the intramuscular injection of the hSGCA-SIIN expressing AAV1 vector, we observed a significant decrease in the levels of hSGCA expressed in the injected muscle ($p < 0.05$ versus AAV1-FILK) to levels undistinguishable from PBS-injected mice (Figure 3I). These data confirm the immunogenicity of the hSGCA in wild-type mice regardless of the expression of the endogenous murine protein. They also indicate that the hSGCA-SIIN transgene is functionally expressed in muscle fibers and represents a tool to measure immune response activation both against SIINFEKL and MHC class I epitopes derived from hSGCA.

Local Changes in Liver T Cell Populations Are Associated with the Suppression of Anti-hSGCA-SIINFEKL Immune Responses

To evaluate whether concomitant liver and muscle transduction was able to prevent the anti-transgene cytotoxic response, we injected C57BL/6J mice intramuscularly with an AAV1 vector expressing hSGCA-SIIN and intravenously with an AAV9 vector expressing the same transgene under the control of a liver-specific promoter (Muscle-Liver group) (Figure 4A). As controls, mice were injected with PBS (Control group), or intramuscularly with an AAV1 vector expressing hSGCA-SIIN (Muscle group), or intravenously with an AAV9 vector expressing the same transgene in hepatocytes (Liver group). One month post-injection, activation of T cells was measured with an IFN-γ ELISPOT assay, showing the formation of positive spots in the Muscle group only ($p < 0.05$ versus all groups; Figure 4B). Similarly, animals receiving the vector intramuscularly (Muscle group) developed a robust anti-hSGCA humoral immune response ($p = 0.0253$ versus Control group; Figure 4C), which was absent in both the Liver- and Muscle-Liver-treated groups. In the Muscle-Liver group, the lack of T cell activation in splenocytes was accompanied by

Fifteen days after treatment, mice were sacrificed, and tissues were collected. (C–E) IFN-γ-ELISPOT performed on splenocytes stimulated with SIINFEKL peptide (C), hSGCA recombinant protein (D), or the RWLRYTQR peptide (E) derived from hSGCA. (F) HPS staining (upper panel; scale bar: 100 μm) and anti-hSGCA (green), CD8 (red), and DAPI (blue) immunostaining (lower panel; scale bar: 50 μm) performed on TA muscle. (G–I) CD8 (G), IFN-γ (H), and hSGCA (I) mRNA measured in TA. Data were expressed as mean ± SD. Statistical analyses were performed by ANOVA in all panels except for (C)–(E), where a Kruskal-Wallis test was used (*$p < 0.05$, as indicated; $n = 4$ per group).

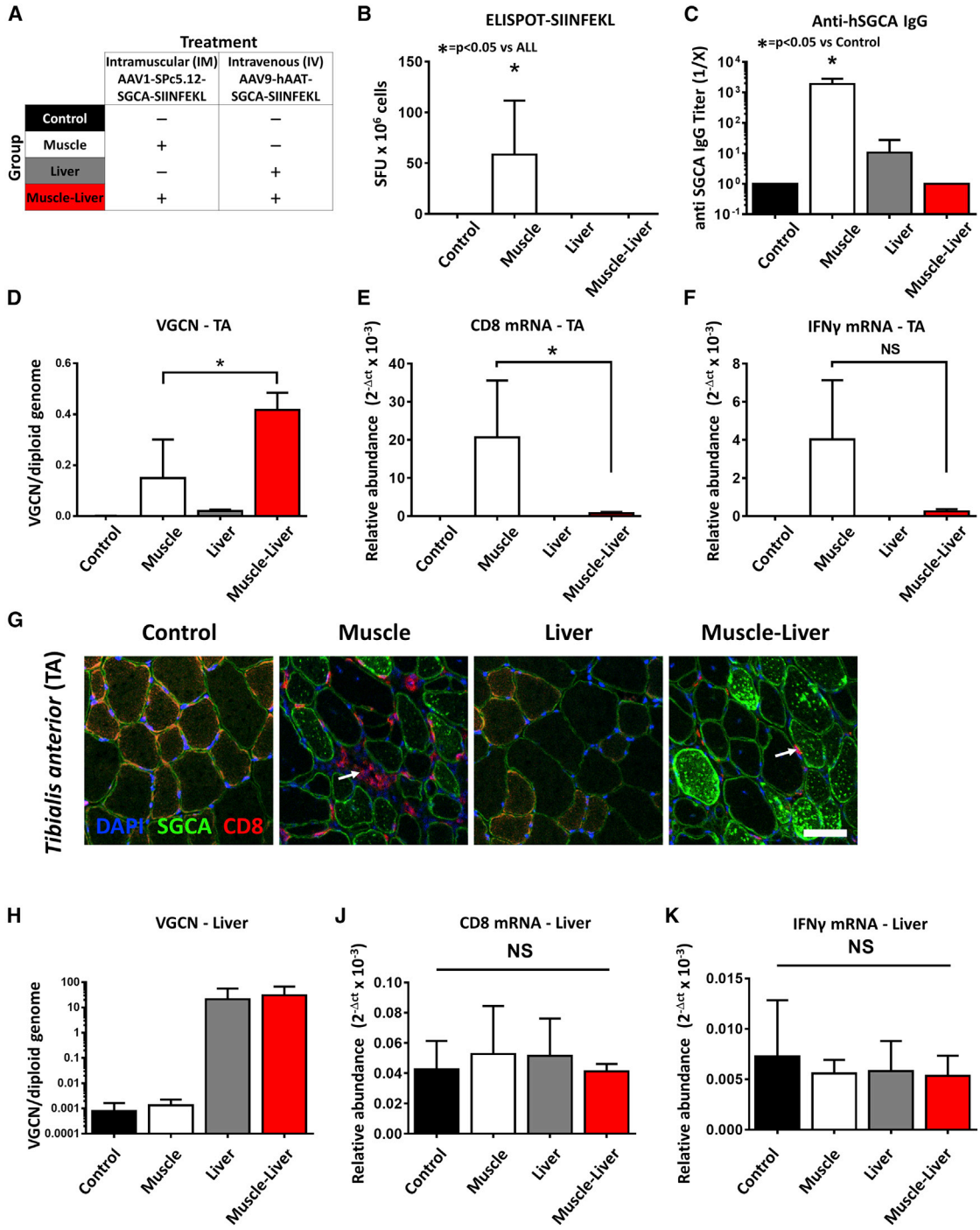

Figure 4. Simultaneous Liver and Muscle Expression of hSGCA-SIINFEKL Controls the Anti-transgene Immune Response

(A) Five-week-old C57BL/6J mice intramuscularly injected (TA) with 1×10^{10} vg/mouse of AAV1-SPc5.12-hSGCA-SIINFEKL vector and intravenously injected with 1×10^{11} vg/mouse of AAV9-hAAT-hSGCA-SIINFEKL (Muscle-Liver group). Two groups of mice received the two vectors separately either by intramuscular (Muscle group) or intravenous (Liver group) injection. PBS-injected mice were used as controls (Control group). One month after treatment, mice were sacrificed, and tissues were collected. (B) IFN-γ-ELISPOT performed on splenocytes stimulated with SIINFEKL peptide. (C) Anti-hSGCA IgG titers measured by ELISA using recombinant hSGCA protein. (D) Vector genome copy number (VGCN) per diploid genome measured in TA. (E and F) CD8 (E) and IFN-γ (F) mRNA measured in TA. (G) Anti-hSGCA (green), CD8 (red), and DAPI (blue)

(legend continued on next page)

an increased number of AAV genome copies in the injected muscle ($p < 0.05$ versus the Muscle group; Figure 4D) and a decreased expression of CD8 and IFN-γ mRNA in the same group ($p < 0.05$ versus the Muscle group for CD8; Figures 4E and 4F). The evaluation of the expression of Treg-signature genes showed increased levels of expression of FoxP3, IL-10, and glucocorticoid-induced TNFR-related protein (GITR) in the Muscle group ($p < 0.05$ versus the Control group; Table S2). Interestingly, the levels of expression of amphiregulin (AREG), a growth factor expressed by muscle Tregs,[19] were increased only in the Muscle-Liver group ($p < 0.01$ versus Control group; Table S2). When we evaluated the expression of hSGCA and the presence of $CD8^+$ T cell infiltrates by immunofluorescence, we confirmed the reduction of infiltrates and the improved muscle transduction in the Muscle-Liver group (Figure 4G). As expected, VGCN analysis in the liver showed similar transduction in the Liver and Muscle-Liver groups (Figure 4H). Notably, no inflammation was observed in the liver after gene transfer as measured by the level of expression of CD8 and IFN-γ mRNA in this tissue (Figures 4I and 4J). The activation of $CD8^+$ T cells was also evaluated in splenocytes by flow cytometry using a SIINFEKL-specific MHC class I dextramer. In the Muscle group, a significant increase in the number of circulating, activated $CD8^+CD44^+$ T cells specific for SIINFEKL was reported ($p < 0.05$ versus all groups; Figures S4A and S4B). Similarly, an increase in $Dextramer^+CD8^+$ cells was observed in non-parenchymal cells extracted from livers of the Muscle group (Table S3). In mice injected with the combination of the two vectors (Muscle-Liver), the number of activated SIINFEKL-specific $CD8^+$ T cells both circulating and infiltrating the liver was undistinguishable from that measured in the untreated control group (Figures S4A–S4E; Table S3). These results indicate that liver transfer of the transgene concomitant to muscle injection controls the anti-hSGCA-SIIN immune response.

Next, based on the RNA expression data in the liver of Muscle-Liver-treated wild-type mice (Table S1) and on published literature on the possible role of Tregs and exhaustion of activated T cells in liver tolerance,[5] we further investigated by flow cytometry the fate of regulatory and effector T cells in the liver of treated animals. We observed a significant increase of $CD4^+FoxP3^+$ Tregs in both Liver and Muscle-Liver groups ($p < 0.05$ versus Control group; Figures 5A and 5B). Interestingly, the levels of $CD8^+$ T cells positive for PD-1 were significantly increased only in the Muscle-Liver group ($p < 0.05$ versus Control group; Figures 5C and 5D), and 18.3% of them were positively stained with the SIINFEKL-specific MHC class I dextramer (Figure S4C; Table S3). Of note, 65% and 56% of PD-1-positive CD8 T cells isolated from livers of the Muscle-Liver group were also positive for LAG3 ($p < 0.01$ versus Control group; Figures 5E and 5F) and TIM3 ($p < 0.05$ versus Control group; Figures 5G and 5H), respectively. Of those cells, between 6% and 8% were positively stained with the SIINFEKL-specific MHC class I dextramer (Figures S4D and S4E). In splenocytes, no changes in Tregs (Figures S4F and S4G), PD-1 $CD8^+$ T cells, or double-positive PD-1/LAG3 and PD-1/TIM3 $CD8^+$ T cells were noted (Figures S4H and S4I).

These data confirm the role of Tregs in the liver-mediated control of the anti-transgene immune response. The simultaneous expression of PD-1/LAG3 and PD-1/TIM3 in liver intraparenchymal, antigen-specific $CD8^+$ T cells observed only in the Muscle-Liver group was associated with the lack of inflammation in the liver. This suggests that the exhaustion of transgene-specific $CD8^+$ T cells, homing to the liver, may play a role in the hepatic control of immune response when immunogenic transgenes are expressed in muscle.

Immune-Checkpoint Blockade Fails to Break Liver-Induced Tolerance

To further investigate the role of T cell exhaustion in liver-mediated control of anti-transgene immunity in muscle, we took advantage of antibodies specifically blocking the interaction between inhibitory co-receptors and their ligands.[30] Specifically, we evaluated the simultaneous blockade of the PD-1/PD-L1 pathway in combination with LAG3 inhibition. C57BL/6J mice, injected intramuscularly with an AAV1 vector expressing hSGCA-SIIN and intravenously with an AAV9 vector expressing the same transgene under the control of a liver-specific promoter, received five intraperitoneal injections of the combination of 200 μg/mouse of anti-PD-1, anti-PD-L1, and anti-LAG3 antibodies (Muscle-Liver+Ab) or five injections of PBS (Muscle-Liver group) at the indicated time points (Figure 6A). Additional controls included mice injected either with PBS (Control) or intramuscularly with AAV1-expressing hSGCA-SIIN (Muscle group). Fifteen days after vector injection, T cell activation was measured by IFN-γ ELISPOT. A significant increase in the number of spots was counted in splenocytes obtained from mice in the Muscle group re-stimulated with SIINFEKL peptide ($p < 0.0001$ versus all groups; Figure 6B). In the Muscle-Liver +Ab group, we observed a slight increase in the spot count, although not statistically significant (Figure 6B). These results were confirmed by flow cytometry using MHC class I SIINFEKL-specific dextramer, which showed a significant increase in the number of $CD8^+CD44^+Dextramer^+$ splenocytes only in mice from the Muscle group ($p < 0.05$ versus all groups; Figures S5A and S5B). In agreement with the ELISPOT results, $CD8^+$ T cell immunofluorescent staining showed a slight increase in T cell infiltrates in muscle of mice of the Muscle-Liver+Ab group (Figure 6C). Similarly, CD8, IFN-γ, and FoxP3 mRNA levels were increased in the Muscle group ($p < 0.05$ versus all groups for CD8; Figures S5C–S5E), whereas a small, not significant, increase was noted in the Muscle-Liver+Ab group (Figures S5C–S5E). No differences were reported in the VGCN between Muscle-Liver and Muscle-Liver+Ab groups (Figure S5F).

immunostaining performed in TA muscle (scale bar: 50 μm). White arrows indicate CD8-positive cells. (H) Vector genome copy number (VGCN) per diploid genome measured in liver. (I and J) CD8 (I) and IFN-γ (J) mRNA measured in liver. Data were expressed as mean ± SD. Statistical analyses were performed by ANOVA in all panels except for (B) and (C), where a Kruskal-Wallis test was used (*$p < 0.05$, as indicated; n = 3 per group).

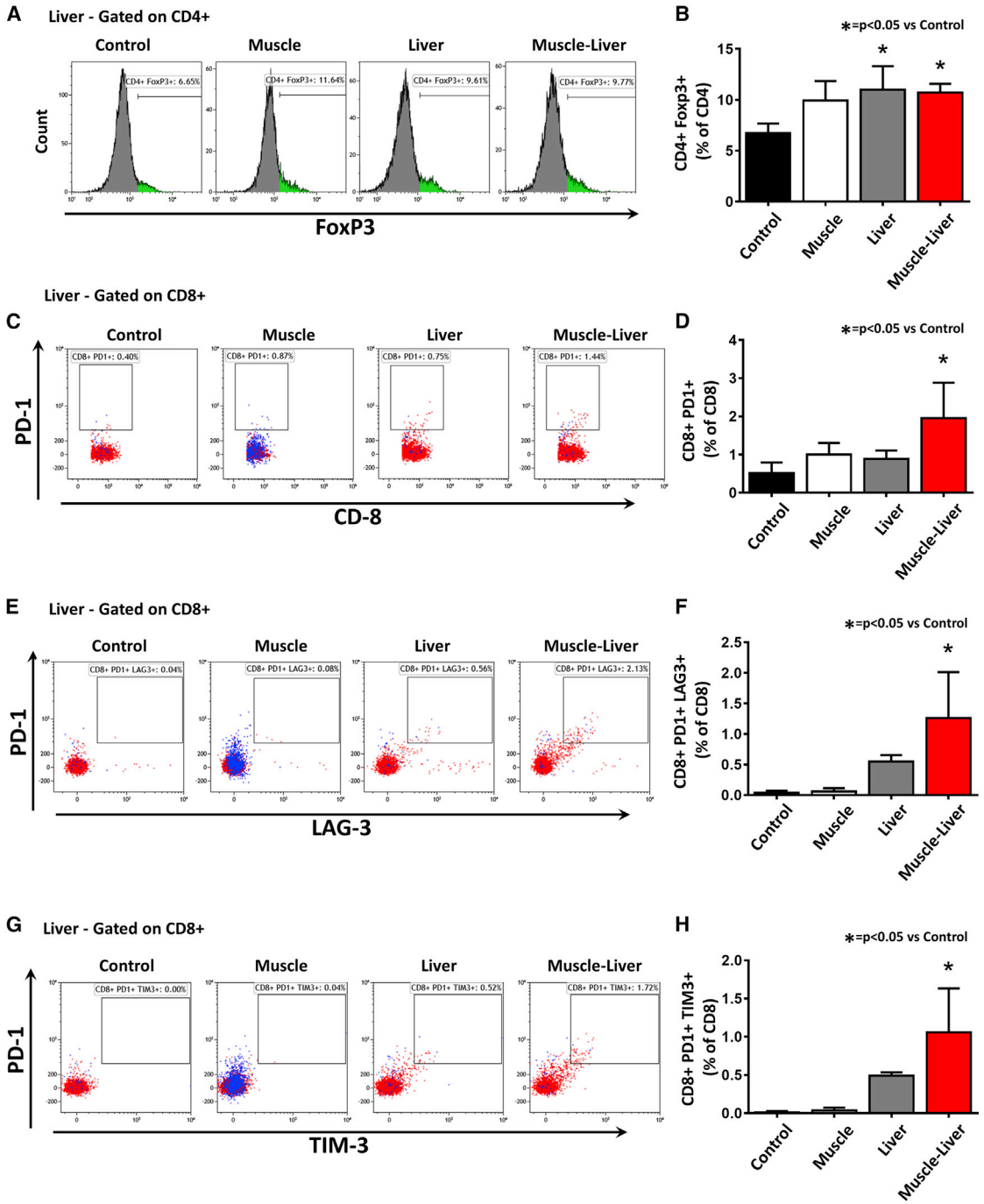

Figure 5. Simultaneous Liver and Muscle Expression of hSGCA-SIINFEKL Increases Liver Intraparenchymal T Regulatory Cells and Exhausted CD8 T Cells

Non-parenchymal cells extracted from livers of mice treated as described in Figure 4 were analyzed by flow cytometry. (A and B) Flow cytometry histograms representing the *CD4*$^+$ *FoxP3*$^+$ population gated on *CD4*$^+$ cells. The histogram shows quantification. (C and D) Flow cytometry dot plots representing the *CD8*$^+$ *PD1*$^+$ population gated on *CD8*$^+$ cells (C). The histogram shows the quantification of the dot plots (D). (E and F) Flow cytometry dot plots representing the *CD8*$^+$ *PD1*$^+$ *LAG3*$^+$ population gated on *CD8*$^+$ cells (E). The histogram shows the quantification of the dot plots (F). (G and H) Flow cytometry dot plots representing the *CD8*$^+$ *PD1*$^+$ *TIM3*$^+$ population gated on *CD8*$^+$ cells (G). The histogram shows the quantification of the dot plots (H). In (C), (E), and (G), the blue dots represent SIINFEKL-specific MHC class I dextramer-stained T cells. Data were expressed as mean ± SD. Statistical analyses were performed by ANOVA (*$p < 0.05$ versus Control; $n = 3$ per group).

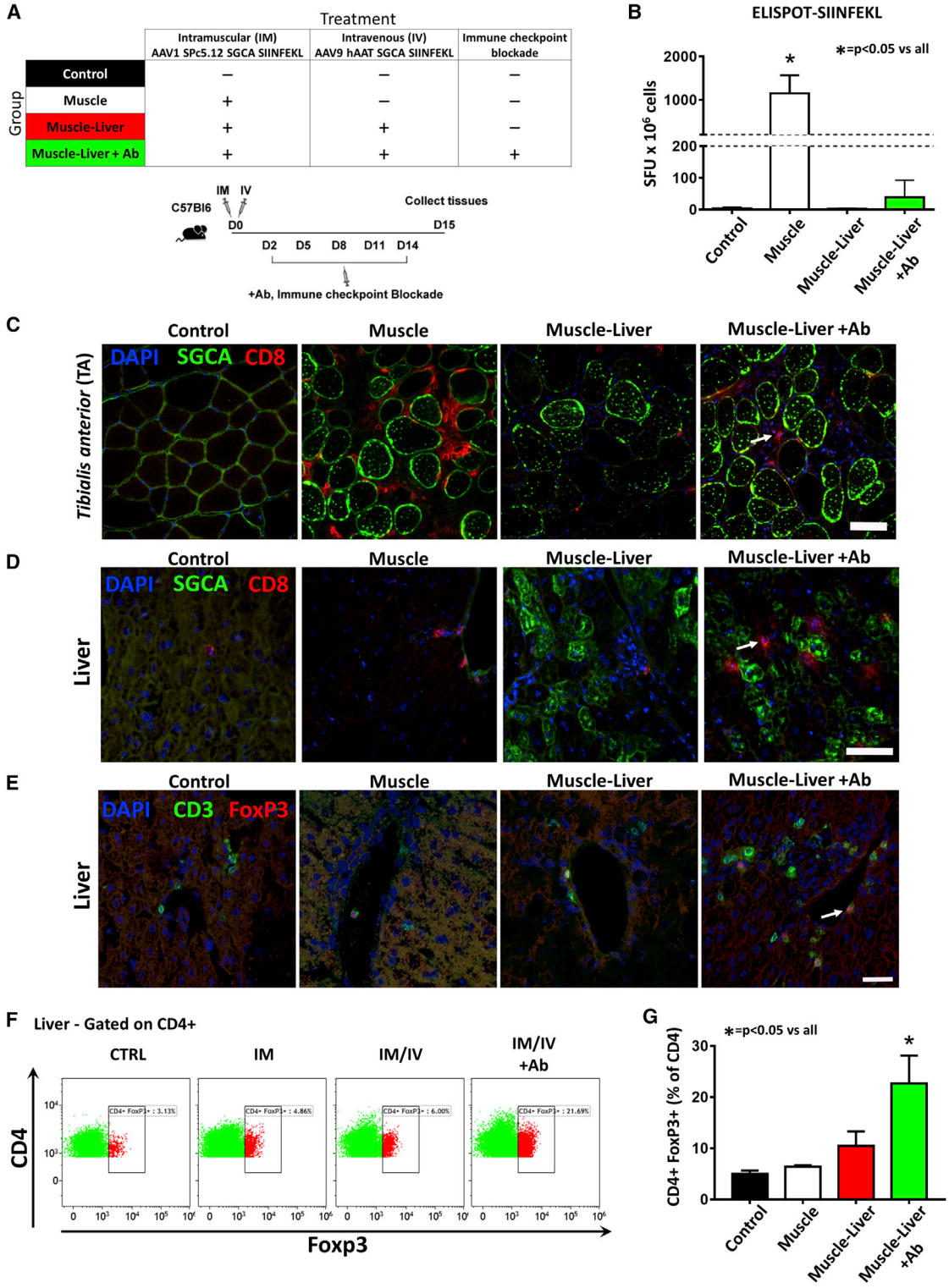

Figure 6. Immune-Checkpoint Blockade Induces Liver Intra-parenchymal Tregs

(A) Five-week-old C57BL/6J mice were intramuscularly injected (TA) with 1×10^{10} vg/mouse of AAV1-SPc5.12-hSGCA-SIINFEKL vector and intravenously injected with 1×10^{11} vg/mouse of AAV9-hAAT-hSGCA-SIINFEKL (Muscle-Liver group). A group of mice treated with the same combination of vectors was treated every 3 days from day

(legend continued on next page)

As expected, anti-hSGCA humoral immune response was significantly increased only in animals receiving the vector intramuscularly (Muscle group versus Control group: $p = 0.0244$; Figure S5G). Animals receiving vectors both in muscle and in liver and treated with the combination of anti-PD-1, anti-PDL-1, and anti-LAG3 antibodies (Muscle-Liver+Ab) showed increased anti-hSGCA humoral immune response compared with the Muscle-Liver group, although the difference did not reach statistical significance.

Analysis of liver T cell infiltrates revealed an increase of $CD8^+$ T cells in Muscle-Liver+Ab animals (Figure 6D) and a significant upregulation of CD8 and IFN-γ mRNA expression ($p < 0.01$ versus all groups; Figures S5H and S5I). Interestingly, this was accompanied by an increase in $FoxP3^+$ T cells detected by immunofluorescence (Figure 6E) and FoxP3 mRNA levels ($p < 0.01$ versus all groups; Figure S5L) in liver. The increase in $FoxP3^+$ T cell infiltrates in the liver in the Muscle-Liver+Ab group was also confirmed by flow cytometry ($p < 0.001$ versus all groups; Figures 6F and 6G).

These results indicate that immune-checkpoint blockade alone was not sufficient to break liver tolerance. They also suggest a compensatory role of Tregs in the liver, possibly accounting for the suppression of effector T cells expanded following immune-checkpoint blockade.

Concomitant Tregs Depletion and Immune-Checkpoint Blockade Restore Anti-SIINFEKL Cytotoxicity and Break Liver Tolerance

To identify any possible synergy between Tregs and T cells exhaustion in the liver-mediated control of the anti-SIINFEKL immune response in muscle, we injected C57BL/6J mice intramuscularly with an AAV1 vector expressing hSGCA-SIIN and intravenously with PBS (Muscle group) or an AAV9 vector expressing the same transgene under the control of the hAAT promoter. Mice received three intraperitoneal injections of an anti-CD25 antibody (250 μg/mouse) for Tregs depletion and five intraperitoneal injections of the combination of 200 μg/mouse of anti-PD-1, anti-PDL-1, and anti-LAG3 antibodies (Muscle-Liver-Treg+Ab) or three intraperitoneal injections of an anti-CD25 antibody at the dose of 250 μg/mouse (Muscle-Liver-Treg) or five injections of PBS (Muscle-Liver) at the indicated time points (Figures 7A and 7B). As expected, in the Muscle group, we observed the largest number of IFN-γ-positive spots as measured by ELISPOT ($p < 0.05$ versus Muscle-Liver group; Figure 7C). Interestingly, a significant increase in the number of IFN-γ-positive spots in splenocytes from mice of the Muscle-Liver-Treg+Ab group ($p < 0.05$ versus Muscle-Liver group; Figure 7C) was observed. At the same time, $CD8^+$ T cell infiltrates were detected in the liver by both flow cytometry and immunofluorescence ($p < 0.05$ versus Muscle-Liver group; Figure 7D and Figure S6A, respectively) in livers. Additionally, a significantly elevated frequency of $CD8^+CD44^+Dex^+$ T cells was detected by flow cytometry in non-parenchymal liver cells extracted from mice of the Muscle and Muscle-Liver-Treg+Ab groups ($p < 0.05$ versus Muscle-Liver group; Figure 7E; Figure S6B). Simultaneous Tregs depletion and PD-1/PDL-1/LAG3 blockade also resulted in decreased vector copies in injected muscle ($p < 0.05$ versus Muscle-Liver group; Figure 7F) and increased $CD8^+$ T cell infiltrates co-localized with fibers expressing the hSGCA transgene, as observed by immunofluorescence (Figure 7G). CD8 and IFN-γ mRNA expression were also significantly upregulated in muscle ($p < 0.05$ versus Muscle-Liver group for CD8; $p < 0.05$ versus Muscle-Liver-Treg group for IFN-γ; Figures S6C and S6D). Accordingly, although the anti-hSGCA humoral response was reduced in mice of the Muscle-Liver and Muscle-Liver-Treg groups ($p = 0.0453$ and $p = 0.0107$ versus Muscle group, respectively), when both Tregs depletion and PD-1/PDL-1/LAG3 blockade were applied, the anti-hSGCA antibodies were not significantly different from the one measured in mice of the Muscle group ($p = 0.2164$ versus Muscle group; Figure S6E). These results demonstrate that Treg depletion alone cannot break an already established tolerance, and that PD-1/PDL-1 and LAG3 acts synergistically with Tregs induction in maintaining liver-dependent anti-transgene tolerance and controlling transgene-specific T cell responses in muscle.

DISCUSSION

Muscle can be considered the hotbed of immune responses, particularly when underlying conditions alter its immune environment.[31] This poses important challenges to the development of gene transfer strategies for the treatment of neuromuscular diseases, particularly for muscular dystrophies, in which continuous muscle breakdown and regeneration trigger inflammation. Here, we dissected the role and mechanisms of liver-mediated control of transgene immune responses induced by muscle-directed gene transfer with AAV vectors. This work highlights the synergy between liver-induced Tregs and inhibitory co-receptors, involved in the control of effector T cell responses, in preventing and reversing cell-mediated transgene immunity in muscle.

Preclinical and clinical results of AAV vector-based gene therapies for neuromuscular disorders indicate that intramuscular delivery of AAV vectors is likely to trigger both humoral and cell-mediated transgene immune responses.[14–17] Several factors contribute to shape the magnitude of these responses; for example, host genetic background,[32] underlying muscle inflammation,[17,33] and pre-existing

2 to day 14 with the combination anti-PD-1, anti-PD-L1, and anti-Lag3 antibodies (Muscle-Liver+Ab group). Another group of mice received only the AAV1 vector intramuscularly (Muscle group). PBS-injected mice were used as controls (Control group). Two weeks after treatment, mice were sacrificed, and tissues were collected. (B) IFN-γ-ELISPOT performed on splenocytes stimulated with the SIINFEKL peptide. (C) Immunostaining with anti-hSGCA (green), CD8 (red), and DAPI (blue) in TA muscle (scale bar: 50 μm). White arrow indicates CD8 cell. (D) Immunostaining with anti-hSGCA (green), CD8 (red), and DAPI (blue) performed on liver (scale bar: 50 μm). White arrow indicates CD8 cell. (E) Immunostaining with anti-CD3 (green), anti-FoxP3 (red), and DAPI (blue) (scale bar: 25 μm). White arrow indicates FoxP3 cell. (F and G) Flow cytometry dot plots representing the liver non-parenchymal $CD4^+$ $FoxP3^+$ population gated on $CD4^+$ cells (F). The histogram shows the quantification of the dot plots (G). Data were expressed as mean ± SD. Statistical analyses were performed by ANOVA except for (B), where a Kruskal-Wallis test was used (*$p < 0.05$ versus all groups; $n = 4$ per group).

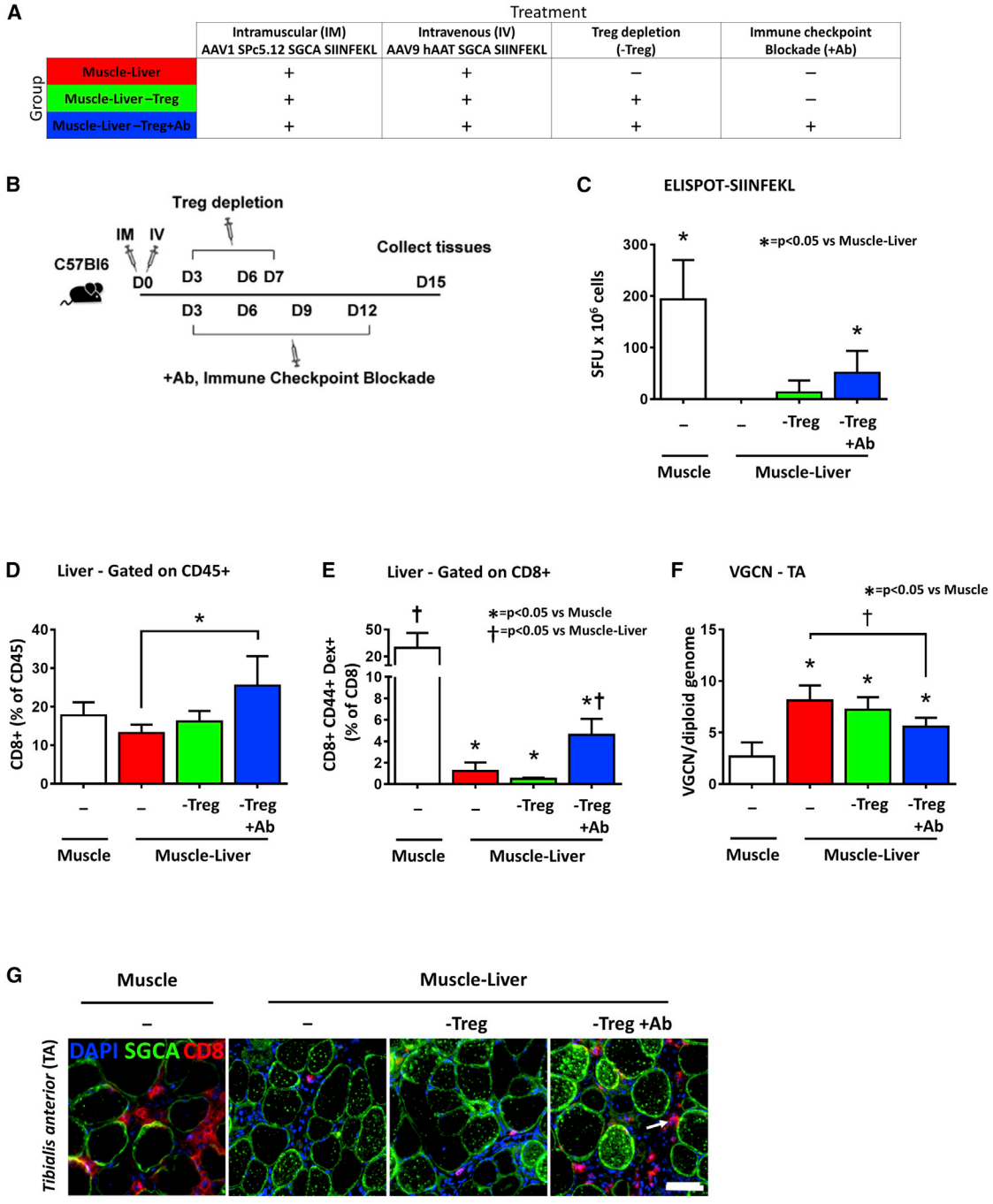

Figure 7. Simultaneous Checkpoint Blockade and Treg Depletion Breaks Liver-Induced Anti-transgene Tolerance

(A and B) Five-week-old C57BL/6J mice were intramuscularly injected (TA) with 1×10^{10} vg/mouse of AAV1-SPc5.12-hSGCA-SIINFEKL vector and intravenously injected with PBS (Muscle group) or 1×10^{11} vg/mouse of AAV9-hAAT-hSGCA-SIINFEKL (Muscle-Liver group). A group of mice treated with the combination of vectors received a simultaneous injection of NAD and anti-CD25 at day 3 and anti-CD25 alone at days 6 and 7 (Muscle-Liver-Treg groups). Finally, another group of mice received the same treatment combined with the injection of anti-PD-1, anti-PD-L1, and anti-LAG3 antibodies every 3 days from days 3 to 12 (Muscle-Liver-Treg+Ab group). Two weeks after treatment, mice were sacrificed, and tissues were collected. (C) IFN-γ-ELISPOT performed on splenocytes stimulated with SIINFEKL peptide. (D) Liver intraparenchymal *CD8*$^+$ cells gated on *CD45*$^+$ cells. (E) Liver intraparenchymal *CD8*$^+$*CD44*$^+$Dextramer$^+$ cells gated on *CD8*$^+$ cells. (F) Vector genome copy number (VGCN) per diploid genome measured in TA. (G) Immunostaining with anti-hSGCA (green), CD8 (red), and DAPI (blue) in TA. White arrow indicates CD8 cell. Data were expressed as mean ± SD. Statistical analyses were performed by ANOVA except for (B), where a Kruskal-Wallis test was used (*$p < 0.05$; $n = 4$ per group).

immunity to the encoded transgene[34] can exacerbate transgene immunity and result in loss of transduced muscle fibers.[17] Interestingly, experience with AAV vector-mediated muscle gene transfer in small- and large-animal models indicates that there is a direct relationship between transgene immunogenicity and route of vector administration. Whereas intramuscular delivery of AAV vectors triggers robust immune responses, systemic vector administration is associated with low to absent anti-transgene immunogenicity.[35,36] Although the outcome of muscle-directed gene transfer could be inferred to differences in antigen presentation in intramuscular versus systemic gene transfer (i.e., local expression of an antigen at high levels via intramuscular vector delivery is more immunogenic than widespread and uniform expression of the same transgene[37]), it is likely that concomitant liver and muscle transduction achieved via systemic vector delivery mediates efficient transgene acceptance.[21,22]

Starting from these observations, and based on the extensive body of work related to hepatic-induced transgene tolerance,[6–8,38–40] here we characterized the mechanisms involved in the control of cytotoxic T cell responses and possibly mediating transgene acceptance after systemic gene delivery.

Liver-mediated induction of immunological tolerance was first described in the context of AAV gene transfer for coagulation factor IX (FIX)[41] and subsequently with other vector platforms[42] and transgenes.[43,44] Interestingly, liver-mediated expression of a transgene has been shown to prevent both humoral and cell-mediated responses triggered by various immunization methods.[22,24,38–41] In the setting of established humoral immune responses, liver expression has been shown to be effective in the eradication of antibodies to FIX and coagulation factor VIII, among other antigens, in both small and large animals.[13,44] Here, we show that liver tolerance is highly effective also in the setting of an ongoing destructive T cell response directed against the transgene, because we were able to rescue transgene expression even when the same transgene was expressed in the liver 2 weeks after the immunogenic intramuscular vector delivery. This is a fundamentally important finding in the treatment of neuromuscular diseases, in particular muscular dystrophies, in which muscle inflammation and pre-existing T cell immunity to the therapeutic transgene can hinder the efficacy of gene transfer.[17,34]

The mechanisms described as mediating hepatic tolerance in the context of AAV gene transfer are multiple,[8,10] although Tregs appear to be key mediators of the suppression of effector T cell responses,[6,7] because depletion of Tregs at the time of gene transfer results in induction of transgene-directed immune responses.[12,45]

The present work, in which the therapeutically relevant transgene α-sarcoglycan was used as a model, supports the hypothesis that effector T cell homing to the liver and their subsequent expression of the checkpoint markers PD-1 and LAG3 on $CD8^+$ T cells is associated with the induction of transgene tolerance and synergistic with the induction of Tregs in controlling anti-transgene immunity. Exhaustion is specifically involved in the control of the immune response when the transgene is expressed in both muscle and liver, and blockade of PD-1 and LAG3 is required to break tolerance. These results are consistent with our recent work in which the ovalbumin model antigen was used to study liver-induced muscle tolerance,[46] and provide additional mechanistic insights on the role of effector T cell homing to the liver and subsequent expression of checkpoint markers for the control of transgene immunogenicity.

Antigen levels in liver play a central role in shaping local immune responses to antigens, as demonstrated in the context of hepatic expression of FIX[41] and ovalbumin.[10,11] As shown here, the fusion of the ovalbumin SIINFEKL epitope, with high affinity for MHC class I, to α-sarcoglycan allowed for the detection of effector T cells by ELISPOT and MHC class I dextramer. Likely due to a bystander effect, it also enhanced the detection of immune responses specific for hSGCA in the ELISPOT assay. Thus, the hSGCA-SIIN fusion represents a tool to monitor transgene-specific immune responses that could be used to develop new strategies to control anti-transgene immune responses in the context of animal models of muscular dystrophies, aimed at improving the safety and efficacy of gene transfer. However, a potential drawback of the strategy used here is that the fusion of immunogenic peptides accelerates the kinetics of the formation of the immune response, and it is likely to modify both the mechanism of tolerance formation and the levels of antigen needed to establish and maintain the peripheral tolerance.

Future work will be aimed at carefully dissecting and comparing the mechanisms involved in the induction of tolerance against hSGCA and hSGCA-SIIN, and at determining the minimal levels of liver expression necessary to prevent muscle-induced transgene immune responses in the context of low- or high- affinity MHC class I epitopes. To this aim, recent work from our lab, in the context of Pompe disease gene therapy, shows that the combination of strong liver promoters with muscle promoters results in good control of anti-transgene immune responses, whereas weaker liver expression fails to control the muscle-driven anti-transgene humoral response.[21]

Reversal of established humoral immunity to a variety of therapeutic transgenes has been demonstrated in small-[47,48] and large-animal[13,44] models of gene transfer. Here, we show the control of an already established $CD8^+$ T cell response against hSGCA mediated by both the induction of Tregs and the homing of transgene-specific $CD8^+$ T cells to the liver, where they express PD-1 and LAG3. The exact mechanism driving homing of reactive $CD8^+$ T cells to the liver remains to be elucidated, although recent work from Paul-Heng and colleagues[49] suggests that direct recognition of antigen expressed in the liver by $CD8^+$ T cells via MHC class I is a key mediator of liver tolerance. Thus, it is conceivable that homing of reactive $CD8^+$ T cells to the liver, via MHC class I recognition of the expressed transgene, together with the unique protolerogenic hepatic immune environment, results in the control of cytotoxic responses via T cell exhaustion. To this end, one interesting and unique finding of the current work is that immune-checkpoint blockade alone is ineffective in breaking liver-induced tolerance. Following the administration of

antibodies against PD-1, PDL-1, and LAG3,[50] given at the time of vector infusion, a slight increase in infiltrating $CD8^+$ T cells was seen in both muscle and liver of animals. At the same time, Tregs were also found in greater number in the same tissues, with no loss of transgene expression of VGCN. This compensatory phenomenon could be explained simply by Tregs homing to the inflamed tissue, like it has been seen in muscle[18,19] and liver,[51] or could simply reflect effect of enhanced proinflammatory signals on Tregs homeostasis.[52] Careful phenotyping of Tregs infiltrates will provide a better understanding of this observation.

The fact that the restoration of transgene immune responses after combined Tregs depletion and checkpoint inhibition blockade was only partial may suggest the existence of additional mechanisms mediating liver tolerance. Alternatively, the anti-CD25 antibody (clone PC-61.5.3) used to deplete Tregs may have affected activated effector T cells expressing the CD25 marker.

The working hypothesis to explain the findings presented here is that, in the absence of liver transduction, $CD8^+$ cells primed in the draining lymph nodes home to the muscle, where they sustain inflammation and clear the transgene expressed in AAV-transduced muscle fibers. Following intramuscular gene transfer, transgene-specific T cells can home to the liver; however, in the absence of transgene expression in hepatocytes, no suppression of the immune response occurs (Figure S7A). When the hSGCA transgene is expressed in the liver, reactive T cells infiltrating the liver are suppressed by the synergistic action of Tregs and upregulation of the inhibitory receptors PD-1/PD-L1 and LAG3. T cells homing to the liver in this case do not participate in the ongoing inflammation in the muscle, and the net result is reduced immune response (Figure S7B). Simultaneous inhibition of the PD-1/PD-L1/LAG3 pathways, together with Treg depletion, lead to the re-activation of exhausted cells that participate in the immune response against the transgene occurring in muscle (Figure S7C). The mechanism proposed represents a simplified model because it excludes the tolerance mechanisms acting locally in the muscle that participate in the control of the anti-transgene immune response.[31]

In conclusion, concomitant liver and muscle expression via AAV vectors allows for efficient prevention and eradication of transgene-specific humoral and cell-mediated immune responses, resulting in long-term transgene expression. Induction of Tregs and effector T cell exhaustion are both key requirements for the effective hepatic control of immune responses. This work provides further insight on the mechanisms of liver-induced immunological tolerance; it also has direct implications on the design of transgene expression cassettes[21] when aiming to treat neuromuscular diseases with underlying muscle inflammation.

MATERIALS AND METHODS

Study Approval

Animal studies were performed in accordance with the current European legislation on animal care and experimentation (2010/63/EU) and approved by the institutional ethics committee of the CERFE in Evry, France (protocol DAP2015-003-A).

Animal Models

The following mouse strains were used: C57BL/6J and $Sgca^{-/-}$ mice. $Sgca^{-/-}$ mice were bred in a pure C57BL/6J background by crossing 10 times in a C57BL/6J background.

AAV-Mediated Gene Transfer

AAV vectors production was performed as already described.[53] Three different serotypes of recombinant AAV1, AAV6, and AAV9 vectors were used to restore α-sarcoglycan expression in muscle of $Sgca^{-/-}$ mice. The use of AAV1 and AAV6 for muscle gene transfer was motivated by their poor humoral cross-reactivity that allowed for 15-day delayed administration of the AAV9 after intramuscular injection of AAV1 and AAV6 (data not shown), and also by the low leakage in circulation of these serotypes after intramuscular administration.[54] The use of AAV9 for liver gene transfer was also justified by the fact that liver transduction with this serotype resulted in efficacy similar to what was observed with AAV8, a classical serotype for liver targeting in both murine models and humans.[55] Viral genomes were quantified by a TaqMan real-time PCR assay using the following primer pairs and TaqMan probes: FWD: 5′-CTCCATCACTA GGGGTTCCTTGTA-3′; REV: 5′-TGGCTACGTAGATAAGTAG CATGGC-3′; probe: 5′-GTTAATGATTAACCC-3′. Mice were injected intravenously into the tail vein with a standard volume of 200 μL of either PBS or AAV9. Intramuscular injections of AAV1 or AAV6 vectors were performed by injection of 25 μL of the diluted vector in the left TA muscle.

Liver Intra-parenchymal Cells and Splenocytes Extraction

Liver intra-parenchymal cells were isolated by mechanical dissociation of the liver tissue and differential centrifugation. In brief, livers were dissociated using a 70-μm cell strainer (Thermo Fisher Scientific, Waltham, MA, USA) and centrifuged for 5 min at 300 × *g* to remove hepatocytes and tissue debris. Supernatants were then centrifuged for 10 min at 500 × *g*. The pellet of this second centrifugation was resuspended in 40% Percoll and overlaid on a 70% Percoll cushion. After centrifugation for 25 min at 1,400 × *g*, the non-parenchymal cells were recovered at the interface between the two layers and used for staining.

Splenocytes were freshly isolated from mouse spleen by mechanical dissociation using a 70-μm cell strainer (Thermo Fisher Scientific, Waltham, MA, USA) and centrifugation for 10 min at 500 × *g* to recover the cells.

Histological and Immunohistochemistry Analyses

Eight-micrometer transversal cryosections were cut from liquid nitrogen-cooled isopentane frozen TA muscles or livers, and stained following classical protocols for histology coloration and immunohistochemistry. Sections were processed for HPS staining as already described and visualized on a Nikon Eclipse E600 microscope (Nikon, Minato, Tokyo, Japan). For immunostaining, unfixed, transverse

cryosections were first blocked with PBS containing 20% fetal calf serum (FCS) for 1 h and then incubated with primary antibodies overnight at 4°C. For the detection of hSGCA-expressing fibers and CD8 T cells, a rabbit polyclonal primary antibody directed against amino acids 366–379 of the hSGCA sequence (AC-ahSarco57; Eurogentec, Seraing, Belgium) and a rat anti-CD8α (Thermo Fisher Scientific, Waltham, MA, USA) were used. For the detection of FoxP3 and CD3-infiltrating cells in liver, TA sections were incubated with rat anti-FoxP3 (eBioscience, Thermo Fisher Scientific, Waltham, MA, USA) and rabbit anti-CD3 antibodies (EPITOMICS; Abcam, Cambridge, UK). After washing with PBS, sections were incubated with a goat anti-rat and goat anti-rabbit secondary antibody conjugated with Alexa Fluor 488 or 594 dyes (Thermo Fisher Scientific, Waltham, MA, USA) for 1 h at room temperature.

After washing with PBS, sections were mounted with Fluoromount-G and DAPI (Southern Biotech, Birmingham, AL, USA), and visualized on a fluorescence microscope (Zeiss Axiophot 2 [Zeiss, Oberkochen, Germany] or Leica TCS-SP8 confocal microscope [Leica, Wetzlar, Germany]).

VGCN, mRNA, and miRNA Quantification in Liver and Muscle Tissues

Genomic DNA was extracted from frozen tissues using the MagNApure kit according to manufacturer's instructions. Vector genome copy number was determined using qPCR from 20 ng of genomic DNA. A serial dilution of a DNA sample of a plasmid harboring one copy of each amplicon was used as the standard curve. Real-time PCR was performed using LightCycler 480 (Roche, Basel, Switzerland) with 0.2 μM of each primer and 0.1 μM of the probe according to the protocol of Absolute QqPCR Rox Mix (Thermo Fisher Scientific, Waltham, MA, USA). The primer pairs and TaqMan probes used for the hSGCA amplification were: FWD: 5′-TGCTGGCCTATGTCATGTGC-3′; REV: 5′-TCTGGATGTCG GAGGTAGCC-3′; and probe: 5′-CGGGAGGGAAGGCTGAAGA GAGACC-3′. The ubiquitous acidic ribosomal phosphoprotein (P0) was used for normalization. Primer pairs and TaqMan probe used for P0 amplification were: FWD: 5′-CTCCAAGCAGATGCAG CAGA-3′; REV: 5′-ACCATGATGCGCAAGGCCAT-3′; and probe: 5′-CCGTGGTGCTGATGGGCAAGAA-3′.

mRNA and miRNA Quantification

Total RNA extraction was performed from frozen tissues by TRIzol (Thermo Fisher Scientific, Waltham, MA, USA). Extracted RNA was dissolved in 20 μL of RNase-free water and treated with Free DNA kit (Ambion) to remove residual DNA. Total RNA was quantified using a NanoDrop spectrophotometer (ND8000 Labtech, Wilmington, DE, USA).

Quantification of microRNAs (miRNAs) was performed using Exiqon miRCURY Locked Nucleic Acid (LNA) Universal RT miRNA PCR (QIAGEN, Venlo, the Netherlands). Total RNA (20 ng) was converted into poly-A primed universal cDNA, and miRNAs were quantified in duplicate for each sample with miRNA-specific LNA primers on the LightCycler 480 (Roche, Basel, Switzerland) following manufacturer's guidelines. Quantification cycle (Cq) values were calculated with the LightCycler 480 SW 1.5.1 using the 2nd DerivLative Max method. qRT-PCR results, expressed as raw Cq, were normalized to the miRNAs identified as the most stable, miR-16 for individual assays in serum and miR-93 in muscle samples. The relative expression was calculated using the $2^{-\Delta Ct}$ method.

For quantification of the transgene expression, 1 μg of RNA was reverse transcribed using the SuperScript II first strand synthesis kit (Thermo Fisher Scientific, Waltham, MA, USA) and a mixture of random oligonucleotides and oligo-dT. Real-time PCR was performed using LightCycler 480 (Roche, Basel, Switzerland) with 0.2 μM of each primer and 0.1 μM of the probe according to the protocol of Absolute QPCR Rox Mix (Thermo Fisher Scientific, Waltham, MA, USA). The primer pairs and TaqMan probes used for the hSGCA amplification were: FWD: 5′-TGCTGGCCTATGT CATGTGC-3′; REV: 5′-TCTGGATGTCGGAGGTAGCC-3′; and probe: 5′-CGGGAGGGAAGGCTGAAGAGAGACC-3′. The ubiquitous acidic ribosomal phosphoprotein (P0) was used to normalize the data across samples. The primer pairs and TaqMan probe used for P0 amplification were: FWD: 5′-CTCCAAGCAGATGCAGCAGA-3′, REV: 5′-ACCATGATGCGCAAGGCCAT-3′; and probe: 5′-CCG TGGTGCTGATGGGCAAGAA-3′. For IFN-γ, CD8, CD4, FoxP3, LAG3, PD-1, PD-L1, PD-L2, TIM3, CTLA4, and 2B4, commercial sets of primers and probes were used (Thermo Fisher Scientific, Waltham, MA, USA). Each experiment was performed in duplicate.

Anti-hSGCA ELISA, ELISPOT, and Cytometry

Anti-hSGCA ELISA, ELISPOT, and cytometry were performed as already described.[56] In brief, blood samples were collected by retro-orbital bleeding and quickly centrifuged for 10 min at 10,000 × *g*. Serum samples were collected and stored at −80°C.

Recombinant hSGCA-GST (Abnova, Taipei City, Taiwan) was dissolved in carbonate buffer and coated to each well of a 96-well plate overnight at 4°C. After washing with PBS containing 0.05% Tween 20 (PBS-T), 3-fold serial dilutions from 1:10 to 1:21,870 of each sera were added to the plate and incubated for 2 h at 37°C. The wells were washed with PBS-T, incubated with a 1:1,000 dilution of horseradish peroxidase (HRP)-conjugated sheep anti-mouse immunoglobulin G (IgG; Southern Biotech, Birmingham, AL, USA) at room temperature for 1 h, washed, and, finally, added with 3,3',5,5'-tétraméthylbenzidine (TMB) agent substrate (Sigma Aldrich, St. Louis, MO, USA). After a 15-min incubation, the reaction was stopped with 1 N sulfuric acid solution. Absorbance values of the plates were read at 405 nm with an Enspire microplate reader. Antibody titer was determined as the last dilution that gives an absorbance value above 0.5.

IFN-γ ELISPOT and IFN-γ ELISA

IFN-γ ELISPOT assay was performed by culturing 2×10^5 splenocytes per well in IFN-γ ELISPOT plates (MAHAS45; Millipore, Molsheim, France). Five peptide epitopes of hSGCA with the highest

probability of presentation by H-2Kb MHC class I molecules were identified by the Immune Epitope Database (http://www.iedb.org) and synthesized by GeneCust. Cells were stimulated either with one of these peptides or with 1 μM hSGCA-GST recombinant protein or with SIINFEKL peptide. As a positive control, cells were stimulated with 5 μg/mL Concanavalin A (Sigma Aldrich, St. Louis, MO, USA). After 24 h of culture at 37°C, plates were washed and the secretion of IFN-γ was revealed with a biotinylated anti-IFN-γ antibody (eBioscience, Thermo Fisher Scientific, Waltham, MA, USA), Streptavidin-Alkaline Phosphatase (Roche Diagnostics, Mannheim, Germany), and BCIP/NBT substrate (Mabtech, Les Ulis, France). Spots were counted using an AID reader (Cepheid Benelux, Leuven, Belgium) and the AID ELISpot Reader v6.0 software. Spot-forming units (SFUs) per million cells were represented after subtraction of background values obtained with unstimulated splenocytes.

IFN-γ secreted by splenocytes stimulated with the recombinant protein hSGCA-GST was measured with the Mouse IFN-gamma Quantikine ELISA Kit (R&D Systems, Minneapolis, MN, USA).

Flow Cytometry Analysis

Single-cell suspensions from spleen and liver were prepared and stained for surface markers with different fluorochrome combinations: anti-CD45 (V450, clone 30-F11; BD Biosciences, San Jose, CA, USA), anti-CD4 (V500, clone RM4-5; BD Biosciences, San Jose, CA, USA), anti-CD8 (AF700, clone 53-6.7; BD Biosciences, San Jose, CA, USA), anti-CD25 (PE-Cy7, clone PC-61.5; BD Biosciences, San Jose, CA, USA), anti-PD-1 (PE-CF594, clone J43; BD Biosciences, San Jose, CA, USA), anti-LAG-3 (PerCP-Cy5.5, clone C9B7W; BD Biosciences, San Jose, CA, USA), anti-TIM-3 (PE-Cy7, clone C9B7W; Thermo Fisher Scientific, Waltham, MA, USA), anti-CD44 (PerCP-Cy5.5, clone IM7; Thermo Fisher Scientific, Waltham, MA, USA), iTAg MHC Tetramer H-2 Kb OVA tetramer-SIINFEKL-PE (MBL, Woburn, MA, USA) followed by cell viability staining using the Fixable Live/Dead kit (BioLegend, San Diego, CA, USA) according to the manufacturer's instructions. Intracellular staining of FoxP3 (antigen-presenting cell [APC], clone FJK-16 s; Thermo Fisher Scientific, Waltham, MA, USA) was performed after fixation and permeabilization using murine FoxP3 buffer kit (Thermo Fisher Scientific, Waltham, MA, USA) according to the manufacturer's instructions. All antibodies were used at one test per 10^6 cells. Samples were acquired using Sony Spectral cell analyzer SP6800 (Sony Biotechnology, San Jose, CA, USA). Data analysis was performed using the SP6800 software (Sony Biotechnology, San Jose, CA, USA) and Kaluza software (Beckman Coulter, Indianapolis, IN, USA).

Statistical Analyses

Statistical analyses were performed using the GraphPad Prism version 6.04 (GraphPad Software, San Diego, CA, USA). Statistical analyses were performed by ANOVA with Tukey's multiple comparison test for all the data except for ELISPOT and ELISA experiments, where a Kruskal-Wallis with Dunn's multiple comparison test was used. In Figure 1, where we compared only Muscle versus Muscle-Liver groups of mice, we used a Student's t test for all the data and a non-parametric Mann-Whitney test for the quantification of anti-hSGCA antibodies by ELISA. Data were expressed as mean ± SD. p values of less than 0.05 were considered statistically significant.

SUPPLEMENTAL INFORMATION

Supplemental Information can be found online at https://doi.org/10.1016/j.omtm.2019.08.012.

AUTHOR CONTRIBUTIONS

G.R., I.R., F.M., and J.P. designed experiments and wrote the manuscript. G.R., J.P., H.C.V., R.H., P.C., and P.S. performed experiments. L.B. and J.D. participated in the discussion of some of the results. F.C. provided reagents. G.R. and J.P. analyzed data. G.R., F.M., and I.R. supervised the project.

CONFLICTS OF INTEREST

All authors declare no competing interests with the content of the current manuscript. F.M. is currently an employee of Spark Therapeutics, Inc., a company involved in the development and commercialization of AAV gene therapies.

ACKNOWLEDGMENTS

This work was supported by the European Union, ERC-2013-CoG Consolidator Grant, grant agreement number 617432 (MoMAAV to F.M.); European Union's research and innovation program under grant agreement no. 667751 (Myocure to F.M.) and 658712 (GLYCODIS3 to F.M. and G.R.); E-Rare2 grant SMART-HaemoCare (to F.M.); ANR-JCJC grant CE18-0014-01 (TRACeGSDIII to G.R.); and the ASTRE laboratories of the Essonne general council grant (to F.M.).

REFERENCES

1. Nathwani, A.C., Reiss, U.M., Tuddenham, E.G., Rosales, C., Chowdary, P., McIntosh, J., Della Peruta, M., Lheriteau, E., Patel, N., Raj, D., et al. (2014). Long-term safety and efficacy of factor IX gene therapy in hemophilia B. N. Engl. J. Med. *371*, 1994–2004.
2. George, L.A., Sullivan, S.K., Giermasz, A., Rasko, J.E.J., Samelson-Jones, B.J., Ducore, J., Cuker, A., Sullivan, L.M., Majumdar, S., Teitel, J., et al. (2017). Hemophilia B Gene Therapy with a High-Specific-Activity Factor IX Variant. N. Engl. J. Med. *377*, 2215–2227.
3. Calne, R., and Davies, H. (1994). Organ graft tolerance: the liver effect. Lancet *343*, 67–68.
4. Rehermann, B., and Nascimbeni, M. (2005). Immunology of hepatitis B virus and hepatitis C virus infection. Nat. Rev. Immunol. *5*, 215–229.
5. Makarova-Rusher, O.V., Medina-Echeverz, J., Duffy, A.G., and Greten, T.F. (2015). The yin and yang of evasion and immune activation in HCC. J. Hepatol. *62*, 1420–1429.
6. Dobrzynski, E., Mingozzi, F., Liu, Y.L., Bendo, E., Cao, O., Wang, L., and Herzog, R.W. (2004). Induction of antigen-specific CD4+ T-cell anergy and deletion by in vivo viral gene transfer. Blood *104*, 969–977.
7. Akbarpour, M., Goudy, K.S., Cantore, A., Russo, F., Sanvito, F., Naldini, L., Annoni, A., and Roncarolo, M.G. (2015). Insulin B chain 9-23 gene transfer to hepatocytes protects from type 1 diabetes by inducing Ag-specific FoxP3+ Tregs. Sci. Transl. Med. *7*, 289ra81.
8. Dobrzynski, E., and Herzog, R.W. (2005). Tolerance induction by viral in vivo gene transfer. Clin. Med. Res. *3*, 234–240.
9. Blackburn, S.D., Shin, H., Haining, W.N., Zou, T., Workman, C.J., Polley, A., Betts, M.R., Freeman, G.J., Vignali, D.A., and Wherry, E.J. (2009). Coregulation of CD8+

T cell exhaustion by multiple inhibitory receptors during chronic viral infection. Nat. Immunol. *10*, 29–37.

10. Kumar, S.R.P., Hoffman, B.E., Terhorst, C., de Jong, Y.P., and Herzog, R.W. (2017). The Balance between CD8$^+$ T Cell-Mediated Clearance of AAV-Encoded Antigen in the Liver and Tolerance Is Dependent on the Vector Dose. Mol. Ther. *25*, 880–891.
11. Tay, S.S., Wong, Y.C., McDonald, D.M., Wood, N.A., Roediger, B., Sierro, F., Mcguffog, C., Alexander, I.E., Bishop, G.A., Gamble, J.R., et al. (2014). Antigen expression level threshold tunes the fate of CD8 T cells during primary hepatic immune responses. Proc. Natl. Acad. Sci. USA *111*, E2540–E2549.
12. Cao, O., Dobrzynski, E., Wang, L., Nayak, S., Mingle, B., Terhorst, C., and Herzog, R.W. (2007). Induction and role of regulatory CD4+CD25+ T cells in tolerance to the transgene product following hepatic in vivo gene transfer. Blood *110*, 1132–1140.
13. Crudele, J.M., Finn, J.D., Siner, J.I., Martin, N.B., Niemeyer, G.P., Zhou, S., Mingozzi, F., Lothrop, C.D., Jr., and Arruda, V.R. (2015). AAV liver expression of FIX-Padua prevents and eradicates FIX inhibitor without increasing thrombogenicity in hemophilia B dogs and mice. Blood *125*, 1553–1561.
14. Herzog, R.W., Mount, J.D., Arruda, V.R., High, K.A., and Lothrop, C.D., Jr. (2001). Muscle-directed gene transfer and transient immune suppression result in sustained partial correction of canine hemophilia B caused by a null mutation. Mol. Ther. *4*, 192–200.
15. Ohshima, S., Shin, J.H., Yuasa, K., Nishiyama, A., Kira, J., Okada, T., and Takeda, S. (2009). Transduction efficiency and immune response associated with the administration of AAV8 vector into dog skeletal muscle. Mol. Ther. *17*, 73–80.
16. Gao, G., Lebherz, C., Weiner, D.J., Grant, R., Calcedo, R., McCullough, B., Bagg, A., Zhang, Y., and Wilson, J.M. (2004). Erythropoietin gene therapy leads to autoimmune anemia in macaques. Blood *103*, 3300–3302.
17. Mendell, J.R., Campbell, K., Rodino-Klapac, L., Sahenk, Z., Shilling, C., Lewis, S., Bowles, D., Gray, S., Li, C., Galloway, G., et al. (2010). Dystrophin immunity in Duchenne's muscular dystrophy. N. Engl. J. Med. *363*, 1429–1437.
18. Villalta, S.A., Rosenthal, W., Martinez, L., Kaur, A., Sparwasser, T., Tidball, J.G., Margeta, M., Spencer, M.J., and Bluestone, J.A. (2014). Regulatory T cells suppress muscle inflammation and injury in muscular dystrophy. Sci. Transl. Med. *6*, 258ra142.
19. Burzyn, D., Kuswanto, W., Kolodin, D., Shadrach, J.L., Cerletti, M., Jang, Y., Sefik, E., Tan, T.G., Wagers, A.J., Benoist, C., and Mathis, D. (2013). A special population of regulatory T cells potentiates muscle repair. Cell *155*, 1282–1295.
20. Gross, D.A., Leboeuf, M., Gjata, B., Danos, O., and Davoust, J. (2003). CD4+CD25+ regulatory T cells inhibit immune-mediated transgene rejection. Blood *102*, 4326–4328.
21. Colella, P. (2018). AAV gene transfer with tandem promoter design prevents anti-transgene immunity and provides persistent efficacy in neonate Pompe disease mice. Mol. Ther. Methods Clin. Dev. *12*, 85–101.
22. Doerfler, P.A., Todd, A.G., Clément, N., Falk, D.J., Nayak, S., Herzog, R.W., and Byrne, B.J. (2016). Copackaged AAV9 Vectors Promote Simultaneous Immune Tolerance and Phenotypic Correction of Pompe Disease. Hum. Gene Ther. *27*, 43–59.
23. Boisgerault, F., Gross, D.A., Ferrand, M., Poupiot, J., Darocha, S., Richard, I., and Galy, A. (2013). Prolonged gene expression in muscle is achieved without active immune tolerance using microRNA 142.3p-regulated rAAV gene transfer. Hum. Gene Ther. *24*, 393–405.
24. Dobrzynski, E., Fitzgerald, J.C., Cao, O., Mingozzi, F., Wang, L., and Herzog, R.W. (2006). Prevention of cytotoxic T lymphocyte responses to factor IX-expressing hepatocytes by gene transfer-induced regulatory T cells. Proc. Natl. Acad. Sci. USA *103*, 4592–4597.
25. Ferrand, M., Galy, A., and Boisgerault, F. (2014). A dystrophic muscle broadens the contribution and activation of immune cells reacting to rAAV gene transfer. Gene Ther. *21*, 828–839.
26. Israeli, D., Poupiot, J., Amor, F., Charton, K., Lostal, W., Jeanson-Leh, L., and Richard, I. (2016). Circulating miRNAs are generic and versatile therapeutic monitoring biomarkers in muscular dystrophies. Sci. Rep. *6*, 28097.
27. Xu, D., and Walker, C.M. (2011). Continuous CD8$^+$ T-cell priming by dendritic cell cross-presentation of persistent antigen following adeno-associated virus-mediated gene delivery. J. Virol. *85*, 12083–12086.
28. John, B., and Crispe, I.N. (2004). Passive and active mechanisms trap activated CD8+ T cells in the liver. J. Immunol. *172*, 5222–5229.
29. Sykulev, Y., Brunmark, A., Tsomides, T.J., Kageyama, S., Jackson, M., Peterson, P.A., and Eisen, H.N. (1994). High-affinity reactions between antigen-specific T-cell receptors and peptides associated with allogeneic and syngeneic major histocompatibility complex class I proteins. Proc. Natl. Acad. Sci. USA *91*, 11487–11491.
30. Anderson, A.C., Joller, N., and Kuchroo, V.K. (2016). Lag-3, Tim-3, and TIGIT: Co-inhibitory Receptors with Specialized Functions in Immune Regulation. Immunity *44*, 989–1004.
31. Boisgerault, F., and Mingozzi, F. (2015). The Skeletal Muscle Environment and Its Role in Immunity and Tolerance to AAV Vector-Mediated Gene Transfer. Curr. Gene Ther. *15*, 381–394.
32. Cohn, E.F., Zhuo, J., Kelly, M.E., and Chao, H.J. (2007). Efficient induction of immune tolerance to coagulation factor IX following direct intramuscular gene transfer. J. Thromb. Haemost. *5*, 1227–1236.
33. Ferrer, A., Wells, K.E., and Wells, D.J. (2000). Immune responses to dystropin: implications for gene therapy of Duchenne muscular dystrophy. Gene Ther. *7*, 1439–1446.
34. Flanigan, K.M., Campbell, K., Viollet, L., Wang, W., Gomez, A.M., Walker, C.M., and Mendell, J.R. (2013). Anti-dystrophin T cell responses in Duchenne muscular dystrophy: prevalence and a glucocorticoid treatment effect. Hum. Gene Ther. *24*, 797–806.
35. Le Guiner, C., Servais, L., Montus, M., Larcher, T., Fraysse, B., Moullec, S., Allais, M., François, V., Dutilleul, M., Malerba, A., et al. (2017). Long-term microdystrophin gene therapy is effective in a canine model of Duchenne muscular dystrophy. Nat. Commun. *8*, 16105.
36. Haurigot, V., Mingozzi, F., Buchlis, G., Hui, D.J., Chen, Y., Basner-Tschakarjan, E., Arruda, V.R., Radu, A., Franck, H.G., Wright, J.F., et al. (2010). Safety of AAV factor IX peripheral transvenular gene delivery to muscle in hemophilia B dogs. Mol. Ther. *18*, 1318–1329.
37. Ge, Y., Powell, S., Van Roey, M., and McArthur, J.G. (2001). Factors influencing the development of an anti-factor IX (FIX) immune response following administration of adeno-associated virus-FIX. Blood *97*, 3733–3737.
38. Cunningham, E.C., Tay, S.S., Wang, C., Rtshiladze, M., Wang, Z.Z., McGuffog, C., Cubitt, J., McCaughan, G.W., Alexander, I.E., Bertolino, P., et al. (2013). Gene therapy for tolerance: high-level expression of donor major histocompatibility complex in the liver overcomes naive and memory alloresponses to skin grafts. Transplantation *95*, 70–77.
39. Lüth, S., Huber, S., Schramm, C., Buch, T., Zander, S., Stadelmann, C., Brück, W., Wraith, D.C., Herkel, J., and Lohse, A.W. (2008). Ectopic expression of neural autoantigen in mouse liver suppresses experimental autoimmune neuroinflammation by inducing antigen-specific Tregs. J. Clin. Invest. *118*, 3403–3410.
40. Lapierre, P., Janelle, V., Langlois, M.P., Tarrab, E., Charpentier, T., and Lamarre, A. (2015). Expression of viral antigen by the liver leads to chronic infection through the generation of regulatory T cells. Cell. Mol. Gastroenterol. Hepatol. *1*, 325–341.e321.
41. Mingozzi, F., Liu, Y.L., Dobrzynski, E., Kaufhold, A., Liu, J.H., Wang, Y., Arruda, V.R., High, K.A., and Herzog, R.W. (2003). Induction of immune tolerance to coagulation factor IX antigen by in vivo hepatic gene transfer. J. Clin. Invest. *111*, 1347–1356.
42. Follenzi, A., Battaglia, M., Lombardo, A., Annoni, A., Roncarolo, M.G., and Naldini, L. (2004). Targeting lentiviral vector expression to hepatocytes limits transgene-specific immune response and establishes long-term expression of human antihemophilic factor IX in mice. Blood *103*, 3700–3709.
43. Sun, B., Bird, A., Young, S.P., Kishnani, P.S., Chen, Y.T., and Koeberl, D.D. (2007). Enhanced response to enzyme replacement therapy in Pompe disease after the induction of immune tolerance. Am. J. Hum. Genet. *81*, 1042–1049.
44. Finn, J.D., Ozelo, M.C., Sabatino, D.E., Franck, H.W., Merricks, E.P., Crudele, J.M., Zhou, S., Kazazian, H.H., Lillicrap, D., Nichols, T.C., and Arruda, V.R. (2010). Eradication of neutralizing antibodies to factor VIII in canine hemophilia A after liver gene therapy. Blood *116*, 5842–5848.
45. Mingozzi, F., Hasbrouck, N.C., Basner-Tschakarjan, E., Edmonson, S.A., Hui, D.J., Sabatino, D.E., Zhou, S., Wright, J.F., Jiang, H., Pierce, G.F., et al. (2007). Modulation of tolerance to the transgene product in a nonhuman primate model of AAV-mediated gene transfer to liver. Blood *110*, 2334–2341.

46. Bartolo, L., Li Chung Tong, S., Chappert, P., Urbain, D., Collaud, F., Colella, P., Richard, I., Ronzitti, G., Demengeot, J., Gross, D.A., et al. (2019). Dual muscle-liver transduction imposes immune tolerance for muscle transgene engraftment despite preexisting immunity. JCI Insight *4*, e127008.

47. Markusic, D.M., Hoffman, B.E., Perrin, G.Q., Nayak, S., Wang, X., LoDuca, P.A., High, K.A., and Herzog, R.W. (2013). Effective gene therapy for haemophilic mice with pathogenic factor IX antibodies. EMBO Mol. Med. *5*, 1698–1709.

48. Han, S.O., Ronzitti, G., Arnson, B., Leborgne, C., Li, S., Mingozzi, F., and Koeberl, D. (2017). Low-Dose Liver-Targeted Gene Therapy for Pompe Disease Enhances Therapeutic Efficacy of ERT via Immune Tolerance Induction. Mol. Ther. Methods Clin. Dev. *4*, 126–136.

49. Paul-Heng, M., Leong, M., Cunningham, E., Bunker, D.L.J., Bremner, K., Wang, Z., Wang, C., Tay, S.S., McGuffog, C., Logan, G.J., et al. (2018). Direct recognition of hepatocyte-expressed MHC class I alloantigens is required for tolerance induction. JCI Insight *3*, e97500.

50. Lichtenegger, F.S., Rothe, M., Schnorfeil, F.M., Deiser, K., Krupka, C., Augsberger, C., Schlüter, M., Neitz, J., and Subklewe, M. (2018). Targeting LAG-3 and PD-1 to Enhance T Cell Activation by Antigen-Presenting Cells. Front. Immunol. *9*, 385.

51. Stross, L., Günther, J., Gasteiger, G., Asen, T., Graf, S., Aichler, M., Esposito, I., Busch, D.H., Knolle, P., Sparwasser, T., and Protzer, U. (2012). Foxp3+ regulatory T cells protect the liver from immune damage and compromise virus control during acute experimental hepatitis B virus infection in mice. Hepatology *56*, 873–883.

52. Grinberg-Bleyer, Y., Saadoun, D., Baeyens, A., Billiard, F., Goldstein, J.D., Grégoire, S., Martin, G.H., Elhage, R., Derian, N., Carpentier, W., et al. (2010). Pathogenic T cells have a paradoxical protective effect in murine autoimmune diabetes by boosting Tregs. J. Clin. Invest. *120*, 4558–4568.

53. Ronzitti, G., Bortolussi, G., van Dijk, R., Collaud, F., Charles, S., Leborgne, C., Vidal, P., Martin, S., Gjata, B., Sola, M.S., et al. (2016). A translationally optimized AAV-UGT1A1 vector drives safe and long-lasting correction of Crigler-Najjar syndrome. Mol. Ther. Methods Clin. Dev. *3*, 16049.

54. Wang, Z., Zhu, T., Qiao, C., Zhou, L., Wang, B., Zhang, J., Chen, C., Li, J., and Xiao, X. (2005). Adeno-associated virus serotype 8 efficiently delivers genes to muscle and heart. Nat. Biotechnol. *23*, 321–328.

55. Vandendriessche, T., Thorrez, L., Acosta-Sanchez, A., Petrus, I., Wang, L., Ma, L., DE Waele, L., Iwasaki, Y., Gillijns, V., Wilson, J.M., et al. (2007). Efficacy and safety of adeno-associated viral vectors based on serotype 8 and 9 vs. lentiviral vectors for hemophilia B gene therapy. J. Thromb. Haemost. *5*, 16–24.

56. Meliani, A., Boisgerault, F., Hardet, R., Marmier, S., Collaud, F., Ronzitti, G., Leborgne, C., Costa Verdera, H., Simon Sola, M., Charles, S., et al. (2018). Antigen-selective modulation of AAV immunogenicity with tolerogenic rapamycin nanoparticles enables successful vector re-administration. Nat. Commun. *9*, 4098.

OMTM, Volume *15*

Supplemental Information

Role of Regulatory T Cell and Effector T Cell Exhaustion in Liver-Mediated Transgene Tolerance in Muscle

Jérôme Poupiot, Helena Costa Verdera, Romain Hardet, Pasqualina Colella, Fanny Collaud, Laurent Bartolo, Jean Davoust, Peggy Sanatine, Federico Mingozzi, Isabelle Richard, and Giuseppe Ronzitti

Supplementary Material

Supplementary Table 1. Inflammatory markers expressed in liver of mice treated as described in Figure 2

	CTRL	IM	IM/IV D0	IM/IV D15
CD4	49.13 ± 11.91	135.73 ± 19.72	36.61 ± 3.63	42.77 ± 14.01
CD8	3.45 ± 1.35	2.55 ± 0.59	15.17 ± 5.31	26.36 ± 18.11
FOX-P3	0.08 ± 0.09	0.06 ± 0.02	0.34 ± 0.13	0.69 ± 0.38
LAG3	1.73 ± 0.92	1.87 ± 0.70	2.63 ± 0.85	4.95 ± 3.14
IFNg	0.78 ± 0.16	0.43 ± 0.12	1.31 ± 0.46	2.00 ± 0.64
PD-1	0.23 ± 0.15	0.15 ± 0.04	2.84 ± 0.93	6.84 ± 5.14
PD-L1	3.40 ± 0.34	1.84 ± 0.32	6.15 ± 1.20	10.45 ± 2.57
PD-L2	0.04 ± 0.02	0.33 ± 0.62	0.08 ± 0.02	0.20 ± 0.06
TIM3	0.94 ± 0.48	0.51 ± 0.02	1.49 ± 0.56	3.05 ± 0.90
CTLA-4	1.43 ± 1.87	0.44 ± 0.39	0.16 ± 0.07	0.49 ± 0.22
2B4	0.34 ± 0.17	0.15 ± 0.06	0.47 ± 0.17	0.77 ± 0.12

Abundancy values ($2^{-\Delta Ct} \times 10^{-4}$) were expressed as mean ± standard deviation. Values in red are significantly different from control Group.

Supplementary Table 2. Inflammatory markers expressed in muscle of mice treated as described in Figure 4

	CTRL	Muscle	Liver	Muscle-Liver
CD4	0.65 ± 0.15	12.95 ± 5.02	0.90 ± 0.24	4.68 ± 0.58
FOXP3	1.15 ± 0.18	4.83 ± 2.39	1.21 ± 0.10	2.41 ± 0.50
IL10	0.02 ± 0.01	0.95 ± 0.49	0.05 ± 0.02	0.50 ± 0.33
IL35	0.29 ± 0.07	0.10 ± 0.01	0.53 ± 0.24	0.28 ± 0.04
GITR	0.20 ± 0.05	9.39 ± 5.43	0.30 ± 0.06	3.71 ± 1.48
CTLA-4	0.0013 ± 0.0005	0.1358 ± 0.1488	0.0021 ± 0.0012	0.0934 ± 0.0770
AREG	0.0005 ± 0.0001	0.0011 ± 0.0007	0.0004 ± 0.0000	0.0178 ± 0.0072

Abundancy values ($2^{-\Delta Ct} \times 10^{-3}$) were expressed as mean ± standard deviation. Values in red are significantly different from control Group.

Supplementary Table 3. Total or Dextramer+ CD8+, CD8+ PD1+, CD8+ PD1+ LAG3+ and CD8+ PD1+ TIM3+ cells measured in liver non-parenchymal cells of mice from the indicated groups.

	CD8+		CD8+ PD1+		CD8+ PD1+ LAG3+		CD8+ PD1+ TIM3+	
Group	Total	Dextramer+	Total	Dextramer+	Total	Dextramer+	Total	Dextramer+
Control	2389 ± 560	44 ± 3	13 ± 10	5 ± 3	1 ± 1	0 ± 0	0 ± 1	0 ± 0
Muscle	3178 ± 1969	527 ± 235	31 ± 16	26 ± 13	2 ± 2	0 ± 0	1 ± 1	0 ± 0
Liver	3538 ± 346	46 ± 14	32 ± 11	6 ± 5	20 ± 6	2 ± 2	17 ± 3	1 ± 1
Muscle-Liver	2860 ± 342	40 ± 6	56 ± 28	9 ± 4	36 ± 22	3 ± 3	30 ± 17	2 ± 1

Absolute counts were reported as mean±standard deviation.

Supplementary FIGURE 1

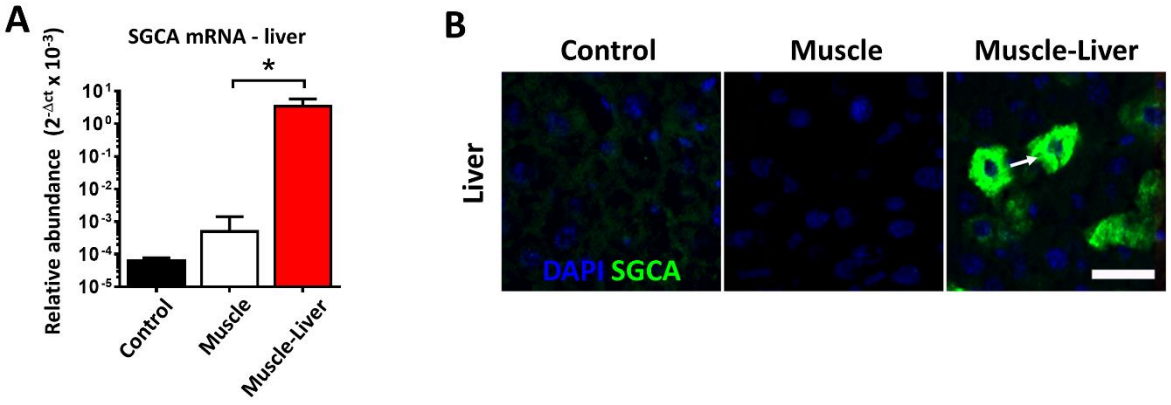

Supplementary Figure 1. (A) hSGCA mRNA measured in liver. **(B)** anti-hSGCA (green), and DAPI (blue) immunostaining performed in liver of mice treated as described in Figure 1 (Scale bar = 25µm). White arrow indicates SGCA-expressing hepatocyte. Data were expressed as mean ± SD. Statistical analysis was performed by t-test (* = $p<0.05$, as indicated, n=4 per group).

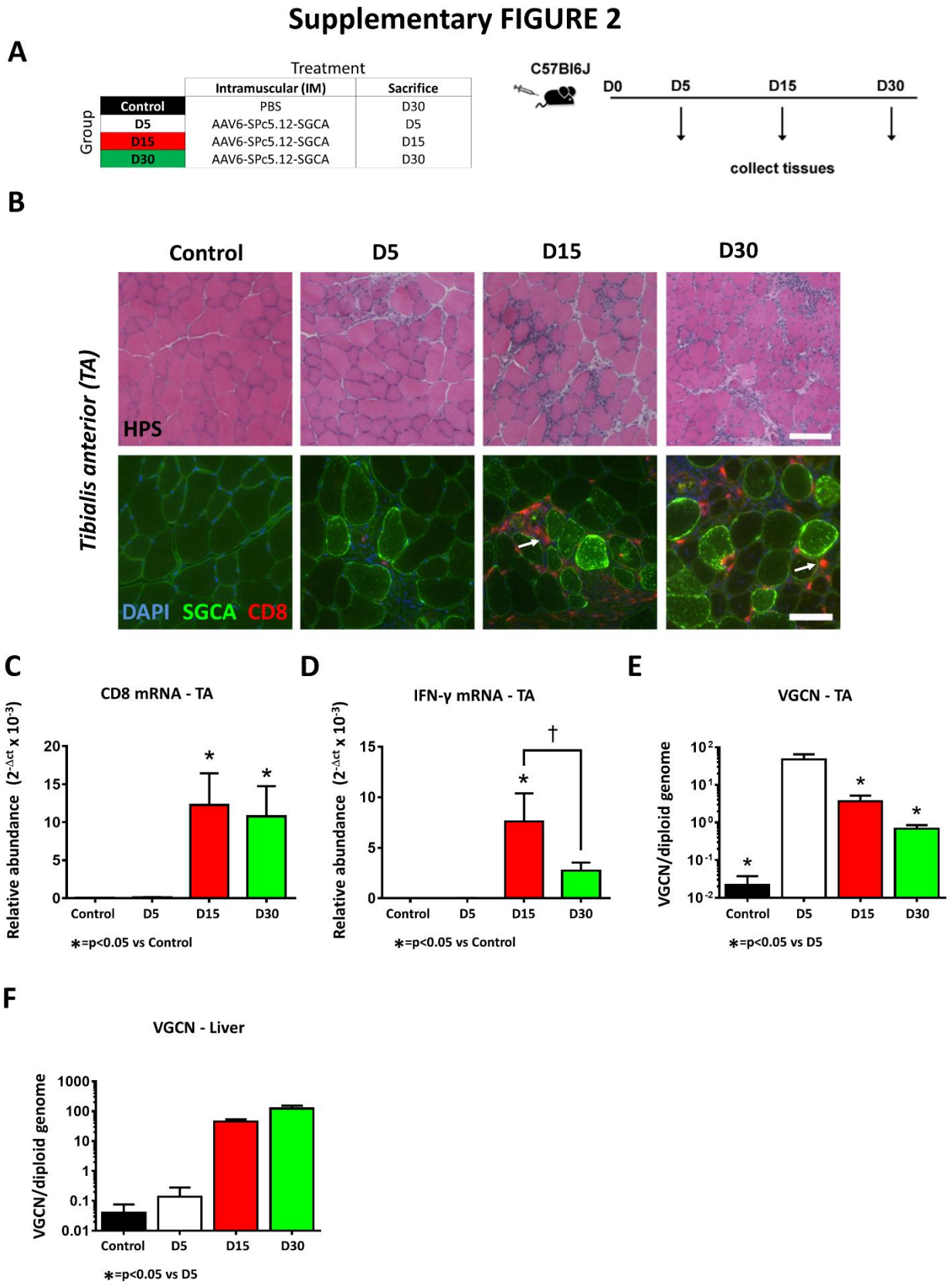

Supplementary Figure 2. (A) Eight-week old C57BL/6J mice received at day 0 an intramuscular injection (IM, *Tibialis Anterior*, TA) of 2.5 x10^9 vg/mouse of AAV6-SPc5.12-

hSGCA vector. Mice were sacrificed and tissues collected at day 0 (D0), day 5 (D5) and day 30 (D30) after vector injection. PBS-injected mice sacrificed 30 days after vector injection were used as controls (Control). (**B)** Hematoxylin phloxine saffron staining (HPS, upper panel, scale bar = 100µm) and anti-hSGCA (green), CD8 (red) and DAPI (blue) immunostaining (lower panel, scale bar = 20µm) performed in TA. White arrows indicate CD8 cells. **(C, D)** CD8 and IFNγ mRNA measured in TA. (**E)** Vector genome copy number (VGCN) per diploid genome measured in TA. (**F)** Vector genome copy number (VGCN) per diploid genome measured in liver. Data were expressed as mean ± SD. Statistical analyses were performed by ANOVA (* = $p<0.05$, † = $p<0.05$ as indicated, n=4 per group).

Supplementary FIGURE 3

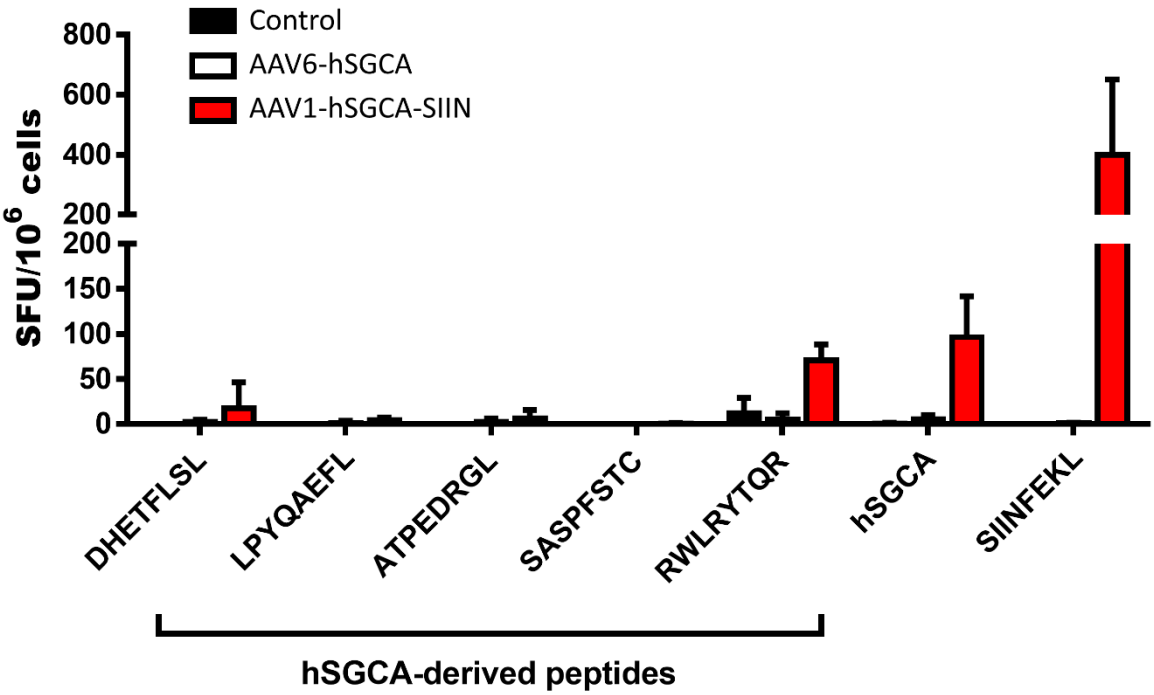

Supplementary Figure 3. Identification of peptide epitopes binding to class I murine MHC in hSGCA protein. Epitopes of hSGCA with the highest probability of presentation by H-2Kb MHC class I molecules were identified by Immune Epitope Database (www.iedb.org). Five peptides with the highest score were synthesized by GeneCust and used to stimulate splenocytes obtained from C57BL/6J mice intramuscularly injected with PBS (Control), AAV6 expressing hSGCA under the control of SPc5.12 promoter (AAV6-hSGCA) or AAV1 expressing hSGCA-SIINFEKL transgene under the control of SPc5.12 promoter (AAV1-hSGCA-SIIN). Splenocytes were stimulated in parallel with hSGCA recombinant protein or with the SIINFEKL peptide. Data were expressed as mean ± SD.

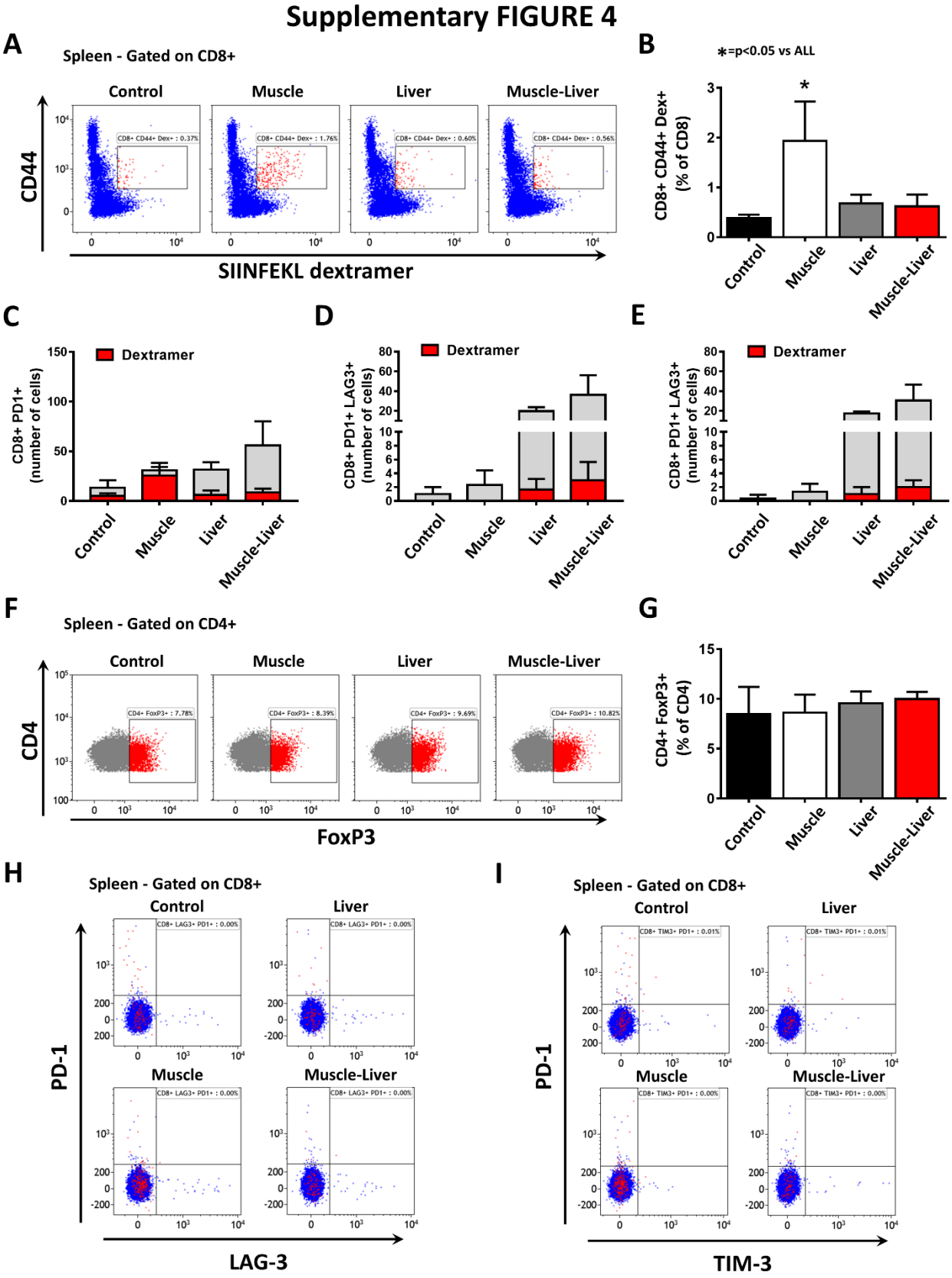

Supplementary Figure 4. (A,B) Flow cytometry dot plots representing CD8+CD44+Dextramer+ cells gated on CD8+ cells in splenocytes. The histogram shows the

quantification of the dot plots. **(C)** Absolute counts of CD8+ PD1+ cells (in gray) and CD8+ PD1+ DEX+ (in red) measured in liver. **(D)** Absolute counts of CD8+ PD1+ LAG3+ cells (in gray) and CD8+ PD1+ LAG3+ DEX+ (in red) measured in liver. **(E)** Absolute counts of CD8+ PD1+ TIM3+ cells (in gray) and CD8+ PD1+ TIM3+ DEX+ (in red) measured in liver. **(F,G)** Flow cytometry dot plots representing CD4+ Foxp3+ cells gated on CD4+ cells in splenocytes. The histogram shows the quantification of the dot plots. **(H)** Flow cytometry dot plots representing CD8+ PD1+ LAG3+ cells gated on CD8+ cells in splenocytes. **(I)** Flow cytometry dot plots representing the CD8+ PD1+ TIM3+ cells gated on CD8+ cells in splenocytes. Data were expressed as mean ± SD. Statistical analyses were performed by ANOVA (* = $p<0.05$, n=3 per group).

Supplementary FIGURE 5

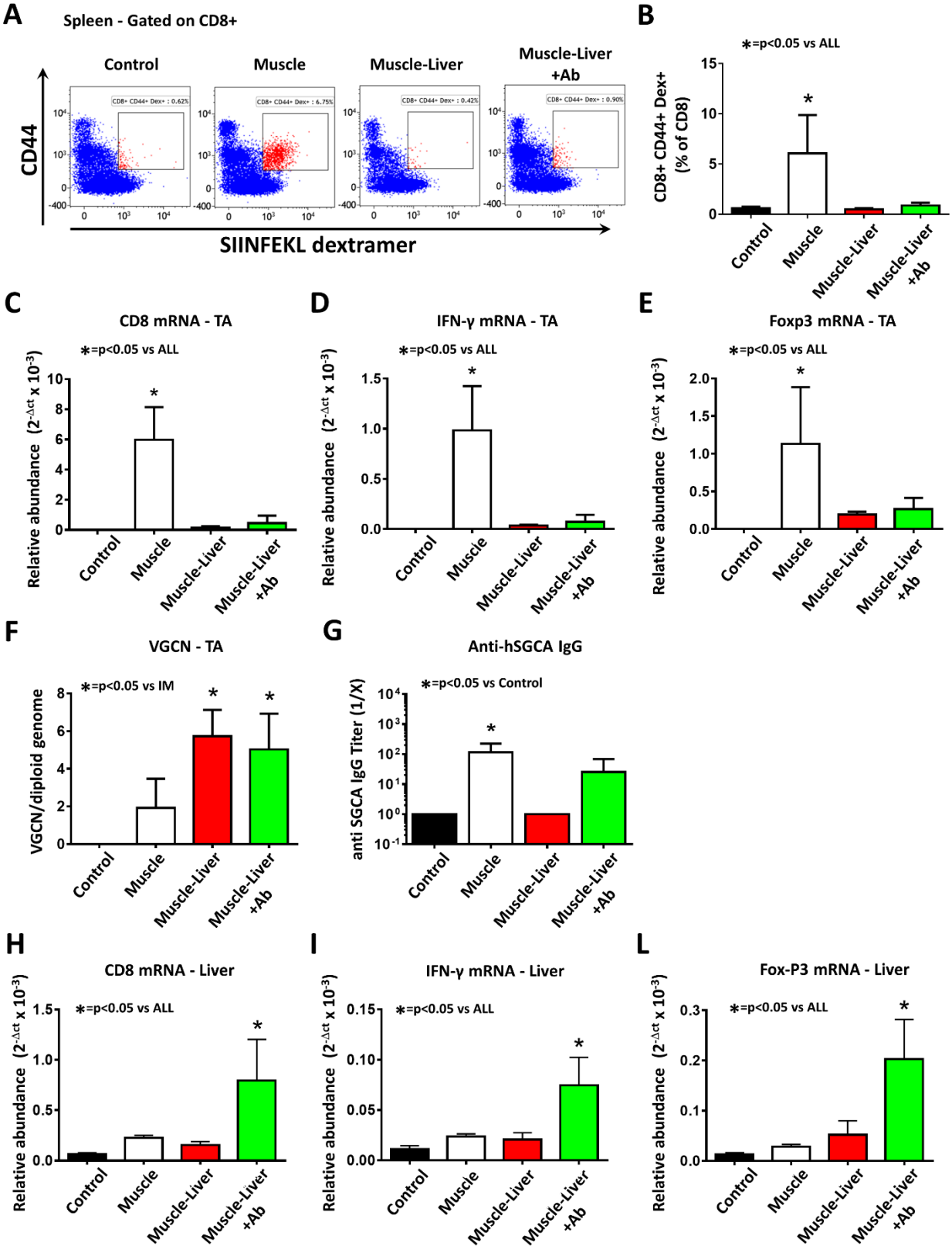

Supplementary Figure 5. (A,B) Flow cytometry dot plots representing CD8+CD44+Dextramer+ cells gated on CD8+ cells in splenocytes. The histogram shows the

quantification of the dot plots. **(C-E)** CD8, IFNγ and FoxP3 mRNA measured in *Tibialis anterior* (TA) muscle. **(F)** Vector genome copy number (VGCN) per diploid genome measured in TA muscle. **(G)** Anti-hSGCA IgG titers measured by ELISA using recombinant hSGCA protein. **(H-L)** CD8, IFNγ and Foxp3 mRNA measured in liver. Data were expressed as mean ± SD. Statistical analyses were performed by ANOVA in all panels except for panel G where a Kruskal-Wallis test was used (* = $p<0.05$, n=4 per group).

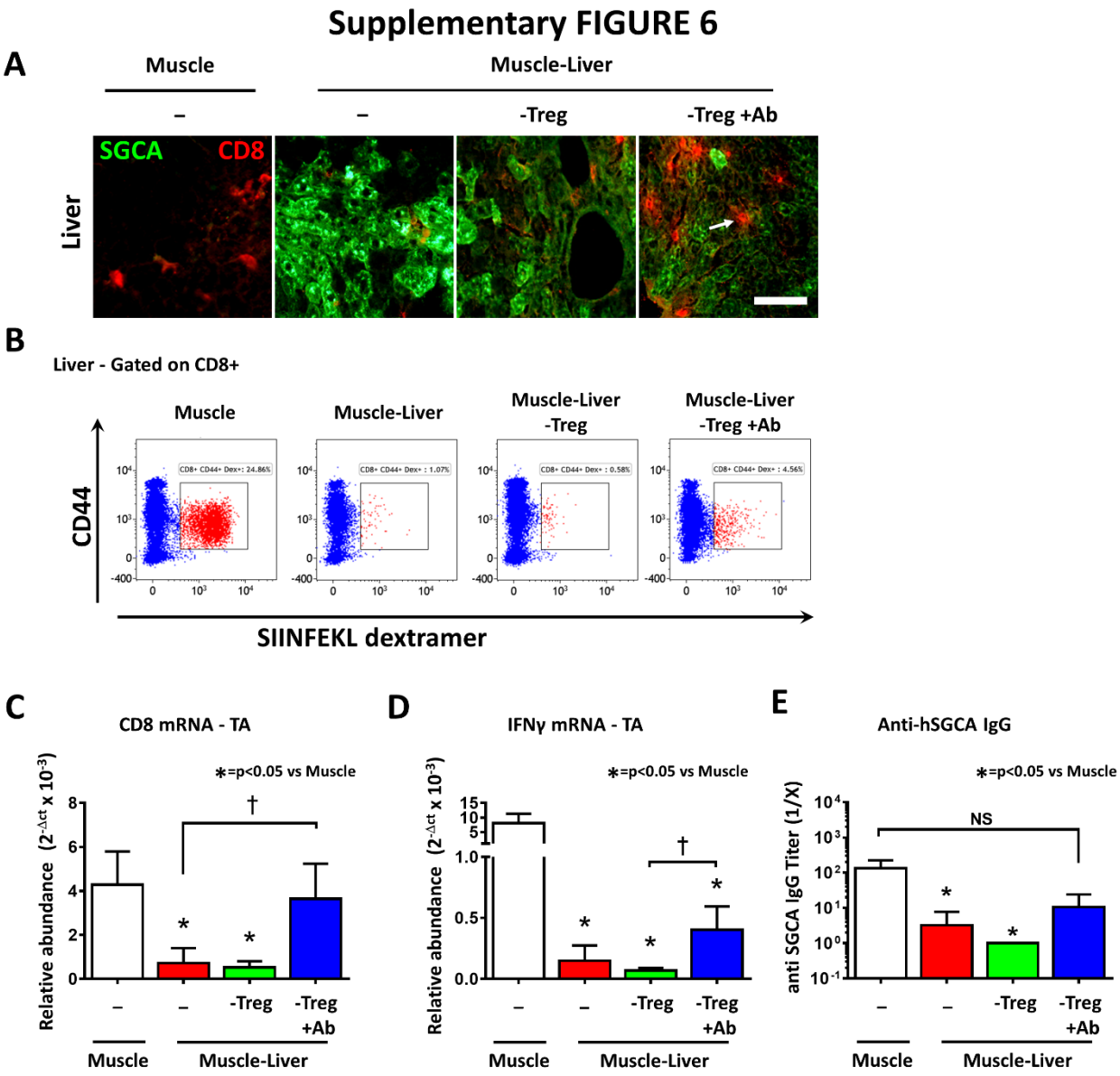

Supplementary Figure 6. **(A)** Immunostaining anti-hSGCA (green), CD8 (red) performed in liver (scale bar = 50 µm). White arrow indicates CD8 cell. **(B)** Flow cytometry dot plots representing liver non-parenchymal CD8+CD44+Dextramer+ cells gated on CD8+ cells. **(C, D)** CD8 and IFNγ mRNA measured in *tibialis anterior*. **(E)** Anti-hSGCA IgG titers measured by ELISA using recombinant hSGCA protein. Data were expressed as mean ± SD. Statistical analyses were performed by ANOVA in all panels except for panel E where a Kruskal-Wallis test was used (* = $p<0.05$, n=4 per group).

Supplementary FIGURE 7

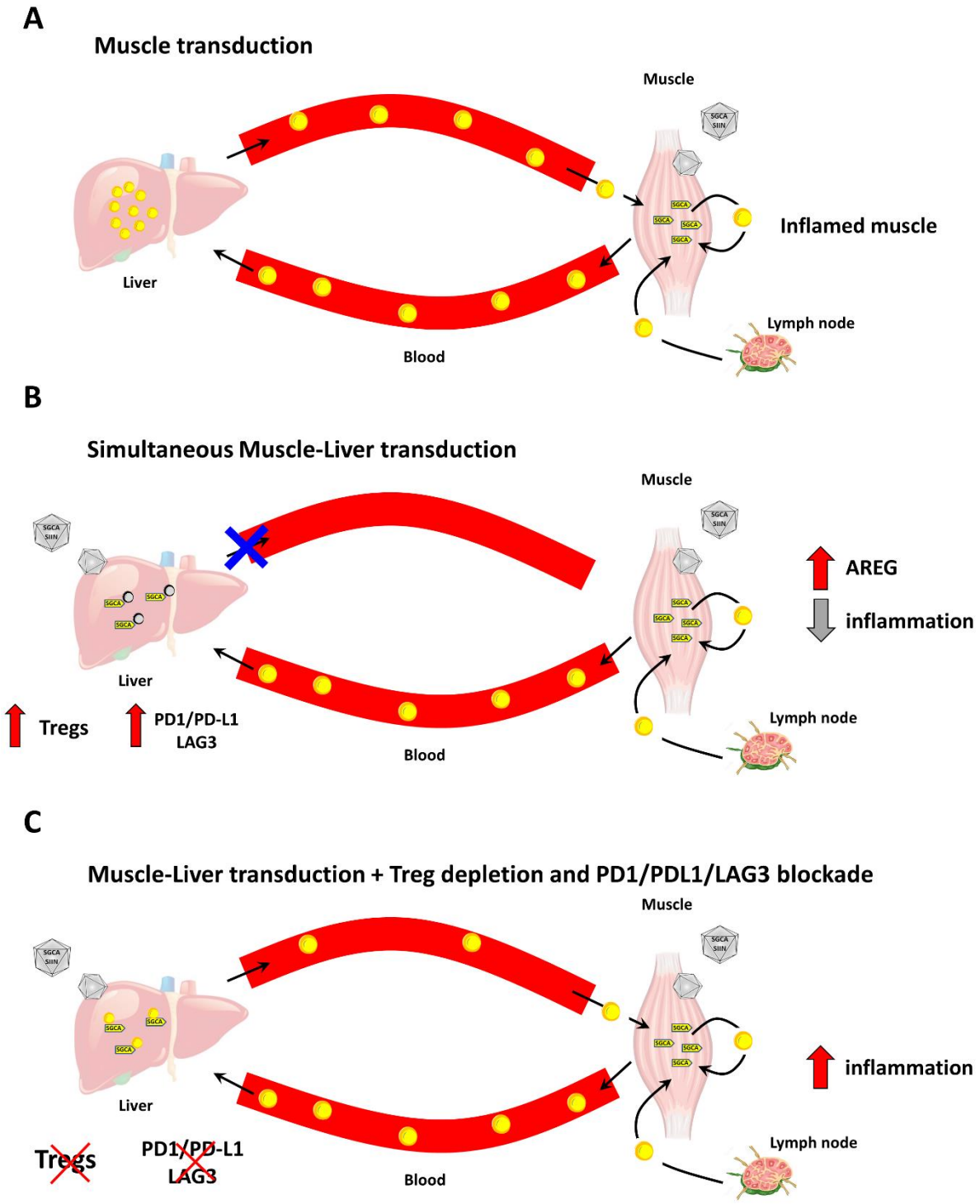

Supplementary Figure 7. (**A**) After intramuscular AAV-mediated delivery of a transgene, antigen presentation occurs directly in muscle or in lymph nodes. Circulating activated T cells

home to the liver with little effect on their activation state. **(B)** In case of simultaneous liver and muscle transduction, activated T cells home to the liver and do not participate in the ongoing immune response in muscle. **(C)** When Tregs depletion is combined with anti PD1/PDL1 and LAG3 inhibition, a partial rescue of the immune response in muscle is observed.